THE HIGH STRAIN-RATE RESPONSE OF POLYURETHANE FOAM AND KEVLAR COMPOSITE

By

Naitram Birbahadur

Submitted in Fulfillment
Of the Requirements for the

Master of Science in Mechanical Engineering

New Mexico Institute of Mining and Technology
Department of Mechanical Engineering

Socorro, New Mexico

May, 2011

ABSTRACT

This research investigates the high strain rate behavior of a sandwiched composite comprised of quick-recovery polyurethane foam and Kevlar. Polyurethane foam is referred to as a material of low mechanical impedance and these materials are widely used as shock absorbers. Researchers at the New Mexico Institute of Mining and Technology have developed this new composite material that can find application in impact loading environments (high strain-rate loading).

Ultimately, one would like to have constitutive relationships for this material that can be used in design tasks of specific devices, especially devices intended for use in impact loading environments. Methods must be found of producing consistent data concerning the material properties under well understood and controlled conditions in order to formulate models of the constitutive properties of materials. No standardized or prescribed tests have been identified for this new fluid-filled, low-impedance polyurethane material being developed at NMT. The work reported in this thesis is an investigation to determine whether using the Split Hopkinson Pressure Bar apparatus, one of the most commonly used pieces of equipment for strain rates between 10^2 s^{-1} and 10^4 s^{-1}, can yield consistent, understandable data for characterizing the material under question at high strain rates. This apparatus is commonly used for testing metals and other high strength, high mechanical impedance materials; however, for valid data some modifications were necessary

when testing materials of low mechanical impedance. If reliable consistent data can be produced from testing the material using this apparatus, then future research may produce the desired constitutive material relationships.

These modifications are discussed and have been completed for investigating this composite material response to high strain rate loading. The investigation was carried out on the core material, and then repeated with the core and different Kevlar skin layers. Some experiments were conducted with fluid in the pores of the core layer, and also some testing at 0^0 C to -80^0 C was carried out. Strain rates between 100 s^{-1} and 2000 s^{-1} were obtained for the core layer and the composite material. It was observed that as the strain rate increased the material's dynamic modulus also increased. The same trend was observed for the fluid filled sandwiched composite.

Keywords: Split Hopkinson pressure bar; composite materials; low impedance materials; high strain rate loading; polyurethane foam.

ACKNOWLEDGEMENTS

I would like to express heartfelt thank you to the following persons whose support and guidance throughout my research made this report possible

1. Dr. Ashok Kumar Ghosh – research and graduate academic advisor for this research opportunity and his guidance throughout my research

2. Dr. Claudia M. D. Wilson – graduate committee and undergraduate academic advisor for her advice and encouragement throughout my graduate and undergraduate studies

3. Dr. Keith Miller – graduate committee member for his patience and support throughout my research

4. Dr. Warren Ostergren – Department chair for his advice and support during my research

5. Dr. Merhdad Razavi – undergraduate professor and advisor

6. Mr. George T. Gray from LANL – for facilitating test in laboratory

7. Mr. Carl M. Cady from LANL– for dedicating his time and sharing his knowledge on the SHPB testing

8. Mr. Carl P. Trujillo from LANL – for his assistance and advice on the Taylor Impact test

9. Mr. Jevan Furmanski from LANL – for his help in conducting experiments on the SHPB

TABLE OF CONTENTS

Page

LIST OF TABLES

LIST OF FIGURES

LIST OF ABBREVATIONS AND SYMBOLS

SHPB	Split Hopkinson Pressure Bar
LANL	Los Alamos National Laboratory
NMT	New Mexico Institute of Mining and Technology
LED	Light-emitting diode
C_0	Elastic wave velocity
l_0	Specimen length
E	Young's Modulus of output bar
A_0	Cross sectional area of output bar
A_s	Cross section of the specimen
ρ	Density of the material
ε	Strain
ε_t	Strain in the output bar (transmitted strain)
ε_r	Reflected strain in the input bar
ε_i	Incident strain in the input bar
$l_{impactor}$	Impactor's length
t_d	Impact duration
dB	Decibel
$\acute{\varepsilon}$	Strain rate
σ	Stress
EMRTC	Energetic Materials Research and Testing Center

CHAPTER 1 INTRODUCTION

1.1. Motivation for Research

The development of the new composite material resulted from a project funded partly by the Office of Naval Research who was interested in a material for a stealth naval platform. After an intense literature review about the characteristics of different materials, researchers at New Mexico Institute of Mining and Technology (NMT) decided that a multifunctional composite material could be developed. The researchers chose quick-recovery polyurethane foam for a core layer and Kevlar for skin layer to form a sandwiched composite (Ghosh et al., 2010). Dr. Ashok K. Ghosh, the lead researcher, applied for patent and the U.S. Patent Office approved his application and granted him patent for the composite material. Researchers carried out various experiments to investigate the characteristics of this new material.

First, they (Ghosh, et al., 2007) examined its acoustic dampening characteristics. The material revealed a 25 percent higher transmission loss than that predicted by acoustic mass law at frequencies between 250 -1000 Hz. Further testing at frequencies between 1 kHz and 10 kHz resulted in transmission loss as high as 135 decibel (dB) (Ghosh, et al., 2007). Researchers then investigated the thermal properties of this composite material. The material demonstrated an induced circulation due to convection (Ghosh et al., 2010). With these encouraging results, researchers (Mathews, 2008, Ghosh et al., 2010) then decided to investigate the material's response to high strain rate loading. The work reported in this thesis is an investigation to determine whether using the Split Hopkinson Pressure Bar (SHPB)

apparatus, one of the most commonly used pieces of equipment for strain rates between 10^2 s^{-1} and 10^4 s^{-1}, can yield consistent, understandable data for characterizing the material under question at high strain rates.

The effects of strain rate on material behavior are of significant importance to researchers and engineers for the purpose of developing constitutive equations and efficiently designing engineering structures that experience high strain rate loadings. There are many different tests that have been develop over time to investigate strain rate effects on material properties and limitations are dictated by the material under investigation.

This research investigates the behavior of a low-mechanical impedance material under high strain rate loading by utilizing the SHPB apparatus which required modifications for obtaining valid experimental data since it was originally designed for testing high strength materials. The theory of the SHPB is well developed and researchers have been utilizing this tool for obtaining strain rate testing between 10^2 s^{-1} and 10^4 s^{-1} with different materials exhibiting different behavior in this strain rate regime. The polymer composite comprised of polyurethane foam and Kevlar developed by researchers at New Mexico Tech is being investigated in this study for its application in energy absorbing and shock isolation environments.

1.2. High Strain Rate Loading

One of the most widely accepted methods of determining material stress-strain characteristics at high strain rates is the SHPB apparatus (Harding, 1979). Bertram Hopkinson conducted dynamic experiments in the early 1900 and discovered that the

dynamic strength of steel is at least twice as high as its low-strain-rate strength. Steel also undergoes a ductile-to-brittle transition when the strain rate is increased (Meyers, 1994). Consequently, researchers and engineers became interested in materials behavior at varying strain rate. Meyers (1994) also agreed that it is important to test different material because their responses vary greatly with strain rate. The new foam-Kevlar composite developed by researchers at New Mexico Tech is expected to exhibit an increase in strength with increasing strain rate. As mentioned previously, foam is an example of a low mechanical impedance material, and these materials use are increasing. Some known applications include protection in crashes and packaging, among others (Chen et al., 2002).

1.3. Low Impedance Materials

Engineering materials such as rubbers and foams are increasingly being used in applications where they are subjected to high strain rate and deformations and as shock and vibration absorbers. Some examples are crushable foams in vehicle interiors for passenger protection during crashes, shock absorption application in electronics packaging, and high performance body armors (Sharma et al., 2002, Chen et al., 2000). These materials have low strength, low mechanical impedance, low wave speed, and are often referred to as soft materials. They are typically good shock mitigation and vibration isolation materials. For efficient engineering application and design, the material response to impact loading needs to be determined through vigorous research and experimentation (Song and Chen, 2004, Kolsky, 1949).

The objective of this research is to investigate the behavior of a low strength, low mechanical impedance, quick-recovery polyurethane foam subjected to impact

3

loading. The polyurethane foam is placed between two Kevlar-epoxy laminas, forming a sandwiched composite material that aims to exploits the excellent shock absorbing nature of polyurethane foam and the high tensile strength of Kevlar fibers.

Composite materials are widely used in today's world and their areas of application continue to expand. They include aerospace, aircraft, automotive, marine, energy, infrastructure, armor, biomedical and recreational applications (Daniel and Ishai, 2006). According to Daniel and Ishai (2006) composites have unique advantages over monolithic materials: high strength, high stiffness, long fatigue life, low density, and adaptability to the intended function of the structure. A thorough understanding of this material's response to applied loading conditions is necessary to adequately design the material for specific applications. Therefore, the behavior of this low mechanical impedance material to impact loading will be investigated utilizing the split Hopkinson Pressure Bar apparatus. With the data obtained, an attempt will be made to establish a framework for the development of a constitutive equation to postulate the materials' behavior under high strain rate loading conditions.

Constitutive equations are mathematical models that characterize individual material and its response to applied loads under specific conditions. They consider the macroscopic behavior resulting from the internal constitution of the material (Malvern, 1969). The literature on this subject is vast and encompasses models for solids and fluids, for elasticity, viscoelasticity, and plasticity, for Newtonian fluid and non-Newtonian fluids, and others. Although the possibilities are endless, any worthwhile constitutive model must be in reasonable agreement with physical observation. Of considerable importance in this regard is the requirement that

constitutive models satisfy the principle of material frame-indifference (Slaughter, 2002). Humphrey (2002) wrote numerous articles on constitutive relations, and suggested that for the formulation of constitutive relations one must follow five basic steps regardless of the approach; these are:

1. Delineate general characteristics of the material behavior,

2. Establish an appropriate theoretical framework,

3. Identify specific functional forms of the relations,

4. Calculate values of material parameters,

5. Evaluate the predictive capability of the final solutions.

A representation or description of the material behavior and characteristics under the conditions of interest is needed to classify whether the material exhibits a fluid-like or a solid-like response. If the response is dissipative, isotropic, isochoric, a thorough understanding of all the characteristics of the material is essential so that the appropriate constitutive relation can be formulated with this knowledge (Humphrey, 2002). Malvern (1969) emphasizes that it is not feasible to write down one equation or a set of equations to describe accurately a real material over its range of behavior because material behavior is very complex when the entire range of possible temperatures and deformations are considered.

Investigating this composite's response to impact loading will result in an understanding of this new material's behavior to determine if it can be used for impact applications. The composite material is comprised of open-cell polyurethane foam sandwiched on both sides by Kevlar fabric bounded together by epoxy resin and

hardener. The investigation was carried out on the SHPB apparatus in the laboratory at the New Mexico Institute of Mining and Technology. A brief introduction of the classical SHPB apparatus, its limitations for testing low strength, low mechanical impedance materials, the modifications necessary for different scenarios, and some basic principles that must be followed for valid test results are briefly discussed in Chapter 2.

CHAPTER 2 LITERATURE REVIEW OF THE SHPB

2.1. The Split Hopkinson Pressure Bar Apparatus

Meyers (1994) states that the split-Hopkinson pressure bar (SHPB) is widely accepted as the testing instrument for strain rates between the ranges of 10^2 to 10^4 s^{-1}. Also referred to as the Kolsky bar, it is the most extensively used experimental configuration to measure the response of materials under high strain rate, and was developed by Kolsky (Zukas, et al., 1982, Owens and Tippur, 2009, Lindholm and Yeakley, 1968). The first person to investigate the propagation of stress pulses in a laboratory scale was Bertram Hopkinson. His apparatus, known as the "Hopkinson pressure bar", consisted of a cylindrical steel bar several feet long, and approximately an inch in diameter held in a horizontal position by four threads (Kolsky, 1963). Upon impact from a projectile or subjecting the bar to contact with an explosive charge, a compression pulse was produced and traveled down the bar. His system was "an application of the simple theory of stress propagation of elastic pulses in a cylindrical bar where the length of the pulse is great compared with the radius of the bar" (Kolsky, 1963). When the diameter of the bar is small compared with the length of the pulse, and the material of the bar is not stressed beyond its elastic proportional limit, the pulse is not distorted as it travels down the length of the bar (Kolsky, 1949, Kolsky, 1963).

The behavior of materials under high strain rate loading has been of interest to engineers and researchers for the purpose of developing constitutive relations for various materials (Sharma et al., 2002, Song and Chen, 2004, Kaisers, 1998, Kolsky, 1949). Figures 1 and 2 below illustrate the setup of the SHPB apparatus which

consists of a gas gun, an impactor bar, an input bar and an output bar. Zukas et al. (1982) recommended that the input and output bars be mounted on Teflon or nylon bushings to assure accurate axial alignment while permitting stress waves to pass without dispersion.
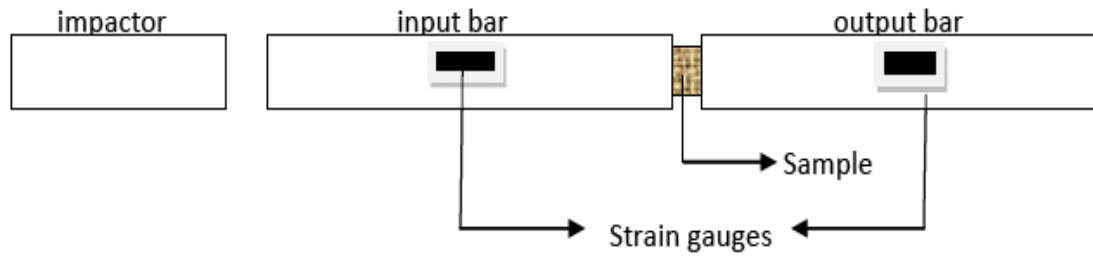
Figure 1: The schematic illustration of the SHPB test setup
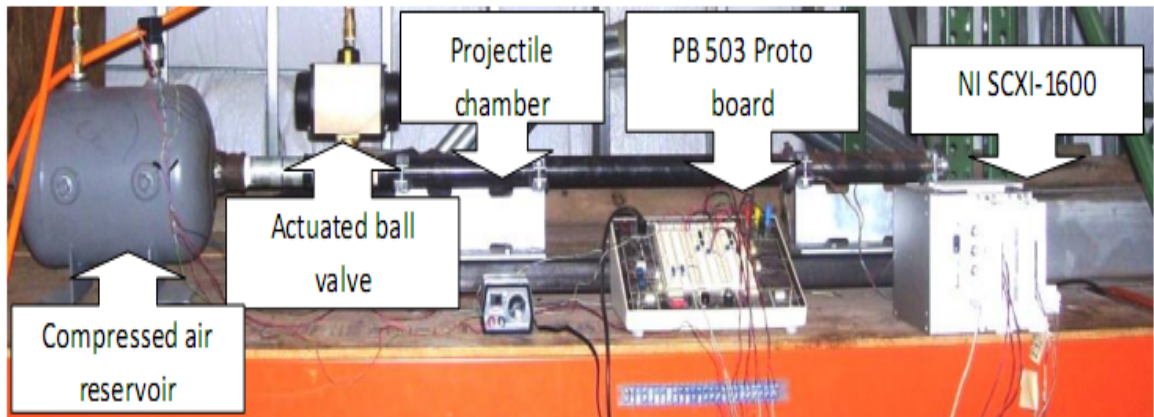
Figure 2: The SHPB in the laboratory at New Mexico Tech

It is also imperative for valid test data that the bars used are straight and free to move without binding and accurately aligned. This accurate alignment is necessary for uniform and one-dimensional wave propagation as well as producing uniaxial compression within the specimen during loading. Restriction on bars' movement will lead to additional noise on the wave measured in the bars (Gray, 2000). The bars of the SHPB apparatus used in the lab at New Mexico Tech are aligned on Teflon bushings as shown in Figure 3, satisfying the alignment and one-dimensional wave propagation criteria.
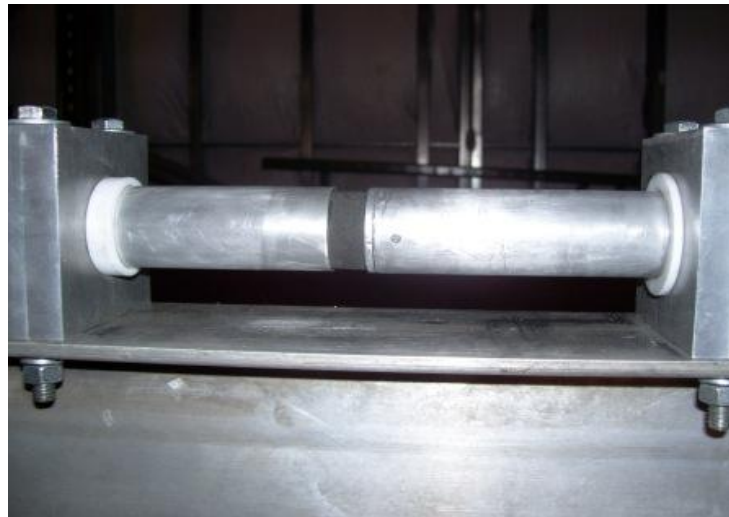
Figure 3: Teflon bushings and the pressure bars

The one-dimensional elastic wave is produced by the impacting bar which strikes the input bar (incident bar) and creates an elastic pulse or longitudinal wave which travels through the input bar, the sample under testing, and the output bar. The incident pulse is measured by the strain gauge mounted on the incident bar. A pulse is then reflected from the interface of the input bar and the sample which is again measured by the strain gauge that is mounted on the incident bar. Thus, the strain

gauge mounted on the incident bar measures both the incident ε_i (t) and the reflected pulses ε_r (t) while the strain gauge on the output bar measures the transmitted strain ε_t (t). Zukas et al. (1982) states that the equations for analyzing stress, strain, and strain rate are based on the assumption that the stresses and velocities at the end of the specimen are propagated down the bars in an un-dispersed manner. The wave-transit time in the short specimen is small compared to the total time of the experiment and many wave reflections can take place back and forth along the specimen. Also, the stress and strain are assumed to be uniform along the specimen (Zukas et al., 1982). When the incident bar is struck by the impacting bar, an elastic wave is produced, the elastic wave deforms the specimen plastically. However, it is important to know that the SHPB should not be considered as plastic wave propagation experiment (Meyers, 1994).

According to Kaiser (1998), the results of the Split-Hopkinson bar experiment can be summarized as follows:

1. The reflected and transmitted waves are proportional to the specimen's strain rate and stress, respectively.

2. By integrating the strain rate generated from the test, the strain in the sample can be determined and,

3. The stress strain properties can be calculated by analyzing the strain in the input and output bars.

The longitudinal wave formed takes the shape shown in Figure 4. The shape of the reflected and transmitted pulses are dependent on the area and mechanical

behavior of the specimen, therefore, testing different materials or specimens will produce pulses that have different shapes and sizes (Zukas et al., 1982).
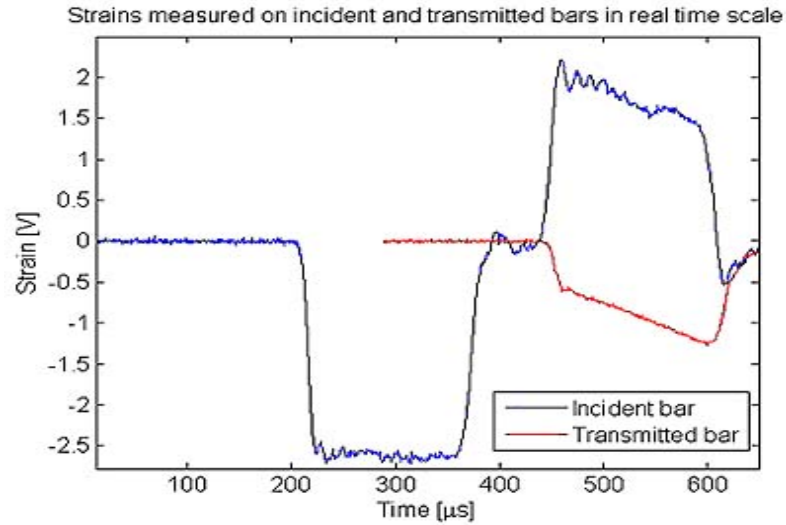
Figure 4: Example of the incident, reflected and transmitted pulses.

2.2. The Theory of the Split Hopkinson Pressure Bar

According to Ninan et al. (2001), the displacement of the incident bar-sample interface $u_I(t)$ is determined by ε_i (t) and ε_r (t), where

$$\varepsilon_i(t) = \varepsilon_I(t - \Delta t) \tag{1}$$

$$\varepsilon_r(t) = \varepsilon_I(t + \Delta t) \tag{2}$$

Δt is the time for the pulse to travel from the strain gauge on the input bar to the sample, t is an instant in time, and ε_I is the strain recorded by the strain gauge in the incident bar at any instant t in time. The strain in the output bar is given by ε_t and ε_r is the strain in the input bar. The displacement u_1 of the input bar and the sample interface is given by Equation (3). Equation (4) gives the displacement at the sample and output bar interface u_2 given by Zukas et al. (1982).

11

$$u_1 = C_0 \int_0^t (-\varepsilon_i + \varepsilon_r)\, dt \qquad (3)$$

$$u_2 = -C_0 \int_0^t \varepsilon_t\, dt \qquad (4)$$

Where C_0 is the longitudinal wave velocity of the bar. The average strain in the sample is given by:

$$\varepsilon_s = \frac{u_2 - u_1}{l_0} = \frac{C_0}{l_0} \int_0^t (-\varepsilon_t + \varepsilon_i - \varepsilon_r)\, dt \qquad (5)$$

Where l_0 is the length of the specimen. The load at the sample interface P_1 and P_2 described by Ninan et al. (2001), and shown in Figure 5, can be determined from the folowing equations:

$$P_1 = A_s E\,(\varepsilon_i + \varepsilon_r) \qquad (6)$$

$$P_2 = A_s E \varepsilon_t \qquad (7)$$

Where A_s is the area of the specimen and E is the elastic modulus of the pressure bars.
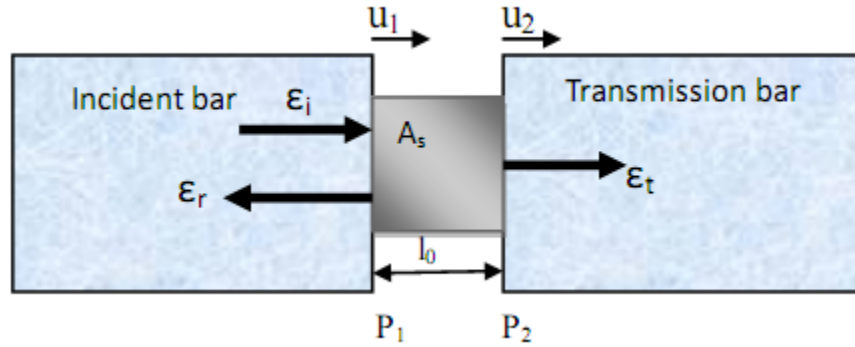
Figure 5: Schematic of the sample-bar interface

Assuming that the pressure difference at each interface of the sample is negligible, then according to Graff (1991), $\varepsilon_t = \varepsilon_i - \varepsilon_r$ and substituting this into Equation (5) gives:

$$\varepsilon_s(t) = -\frac{2C_0}{l_0} \int_0^t \varepsilon_r\, dt \qquad (8)$$

which represents the sample average strain. The stress can be obtained directly from the transmitted strain as given in Equation (9). The strain rate in the speciment is given by Equation (10).

$$\sigma_s = E \frac{A_0}{A_s} \varepsilon_t \tag{9}$$

$$\acute{\varepsilon}_s = \frac{-2C_0}{l_0} \varepsilon_r \tag{10}$$

Where

A_0 is the cross sectional area of the output bar

A_s is the cross sectional area of the specimen

σ_s is the stress in the specimen

$\acute{\varepsilon}_s$ is the strain rate of the specimen

Graff (1991) also stated that in practice, the sample average strain can be obtained by directly integrating the reflected strain and the stress can be obtained directly from the transmitted strain. The stress, strain, and strain rate are average values, and they are determined by assuming uniaxial stress state in the specimen (Zukas et al., 1982).

Traditionally, the SHPB is used to investigate material behavior under dynamic loading conditions. It is commonly used for testing metals, concrete, and ceramics (Chen, et al., 2000). The Split Hopkinson pressure bar can also be used to test composite materials. According to Ninan et al. (2001) there has been a few but relatively recent attempts to systematically model the rate-dependent deformation of composite laminates beyond the elastic region.

This apparatus can also be used to investigate behavior of low strength, low mechanical impedance materials. However, the proper modifications are necessary to obtain reliable data.

2.3. Modifications on the SHPB Apparatus for Testing Low Strength, Low Mechanical Impedance Materials

With a few adjustments, the SHPB can also be used to determine high strain rate behavior of low mechanical impedance materials. With these materials, the incident bar-specimen interface moves almost freely under stress wave loading because most of the incident pulse is reflected back into the incident bar and a very small signal is transferred to the transmission bar (Chen et al., 1999). One method proposed for increasing the signal strength is using a hollow transmission bar (Chen et al., 1999). An X-cut quartz crystal disk embedded in a solid transmission bar (Chen et al., 2000) is also another method of obtaining an amplified transmitted signal. Pulse shaping technique is also another modification (Johnson et al., 2009).

2.3.1. Embedded Quartz Crystal

Chen et al. (2000) suggested that, for increasing the signal in the transmission bar when testing low mechanical impedance materials a circular piezoelectric transducer (an X-cut quartz crystal disk) should be embedded in the middle of a solid aluminum transmission bar of the same diameter to directly measure the time-resolved transmitted force. The X-cut quartz is much more sensitive in detecting forces in its x-direction than the indirect surface strain gauge method. The mechanical impedance of the self-generating quartz transducer is also very close to the mechanical impedance of the aluminum transmission bar. This ensures that

14

introduction of the quartz disk does not affect the one-dimensional wave propagation in the transmission bar (Chen, et al. 2000).

2.3.2. Hollow Transmission Bar

Researchers at the University of Arizona (Chen et al., 1999) have proposed other modifications for the testing of low mechanical impedance materials. They suggested that a high-strength aluminum alloy should be used for the incident bar and a hollow aluminum tube should be used for the transmission bar. The hollow aluminum tube will cause an increase in σ_s according to Equation (9). Also, the hollow tube will produce an increase in the transmitted signal amplitude (Chen et al., 1999). The SHPB apparatus in our experiment utilizes 6061-T6 aluminum bars; one hollow transmission bar and one solid incident bar. The transmission bar has an outer diameter of 31.78 mm and is 6.35 mm thick. The solid incident bar has a 31.75 mm diameter.

Although the principles are the same when using solid or hollow pressure bars, the theory for determining the strain in the specimen when using hollow bars is different. Chen et al. (1999) developed an equation for determining the strain for low impedance materials using hollow transmission bars. They suggested that according to Equation (9), the stress is a function of the transmitted stain $\varepsilon_t(t)$ and therefore in order to increase $\varepsilon_t(t)$ under the same stress level either the area of the output bar A_0 or the Modulus E should be reduced. Using a hollow bar will result in a smaller A_0 and using low impedance bar material with a lower elastic modulus will cause an increase in the transmitted stain $\varepsilon_t(t)$. The hollow bar must be fitted (press fitted) on

the end with a cap of the same bar material at the bar-specimen interface (Chen et al., 1999). From intuition, one might believe that the end cap will interfere with the stress pulse passing through the bar. However, the researchers (Chen et al., 1999) stated that using a pulse shaper to obtain a significant increase in the rise time of the loading pulse and filtering out high-frequency components in the waveform, the effect of the end cap can be neglected. Pulse shaping techniques will be discussed in Section 2.3.3. Chen, et al. (1999) stated that by using a hollow aluminum bar of 19 mm outer diameter and 1.5 mm wall thickness, the transmitted signal is amplified 10 times as compared to using solid steel bars. This is from the combined effect of the lower Elastic modulus and the ratio of A_0/A_s of the hollow aluminum bar.

To further increase the amplitude of the transmitted signal, transmission bars with thinner walls can be used. Chen et al. (1999) also proposed a modification of the theory to determine the strain in the specimen. When the specimen is in equilibrium, Equations (6) and (7) are equal, and yield

$$\varepsilon_t = \frac{A_i}{A_t}(\varepsilon_i + \varepsilon_r) \tag{11}$$

Where A_i and A_t are the cross-sectional areas of the incident and transmission bars respectively, and substituting equation (11) into equation (5) gives the strain in the specimen as

$$\varepsilon_s = \frac{C_0}{l_0}\left(1 - \frac{A_i}{A_t}\right)\int_0^t \varepsilon_i(t)dt - \frac{C_0}{l_0}\left(1 + \frac{A_i}{A_t}\right)\int_0^t \varepsilon_r(t)dt \tag{12}$$

Equation (12) is used to calculate the strain in the specimen from the measured incident and reflected pulses when a hollow transmission bar is used. This equation is

16

quite different from Equation (8) which is used in the classical SHPB test with bars of same cross-sectional areas (Chen et al., 1999).

2.3.3. Pulse Shaping

Pulse shaping technique is another approach that is used to facilitate the testing of low impedance materials (Johnson et al., 2009). It is used to produce a slowly raising incident pulse, which is necessary to minimize the effect of dispersion of the wave in the bars and to allow the sample to achieve dynamic stress equilibrium (Frew et al., 2005) which is necessary in SHPB testing (Song and Chen, 2004). For dynamic stress equilibrium, the loading pulse must stress the front and the back faces of the specimen almost simultaneously. In testing soft materials, this can be achieved by pulse shaping (Chen et al., 1999). The incident pulse can be shaped by two methods, by machining a larger radius on the impactor face or by placing a tip material between the input bar and the impactor which can be made of any material such as aluminum, brass, paper, or stainless steel, in the shape of a disk slightly larger than the bars (Frew et al., 2005). A nearly constant strain rate in a sample can be generated by choosing the proper pulse shaper (Chen et al., 1999, Frew et al., 2005). The pulse shaping technique is used to decrease the initial incident loading rate by increasing the rise time of the incident pulse (Song and Chen, 2005).

A simple pulse shaping technique for testing low impedance materials involves attaching a polymer disk with a thin layer of vacuum grease to the impact end of the incident bar. The polymer disk will deform plastically upon impact and effectively increase the rise time of the pulse (Chen et al., 1999). Also, on the impact surface of the polymer disk, attaching two layers of tissue paper using vacuum grease

will filter out high-frequency components in the incident pulse (Chen et al., 1999).

This method was used in this investigation because it was found to be effective for

this new material; previous researchers have utilized this technique with great success

(Mathews, 2008).

The amplitude and duration of the incident pulse can be controlled by varying

the striker bar velocity and length, respectively (Chen et al., 1999). According to

Meyers (1994), the impact duration t_d is determined from the following equation:

$$t_d = \frac{2l_{impactor}}{C_0} \tag{13}$$

Where $l_{impactor}$ is the impactor length and C_0 is the elastic wave velocity. This equation

is valid only if the impactor and the input bars are of the same materials. So from

Equation (13), the duration of the incident pulse can be increased by increasing the

length of the impactor. The amplitude of the incident pulse is directly related to the

impactor velocity since it produces the compressive wave in the input bar. The

particle velocity U_p is parallel to the wave velocity for longitudinal wave, as in the

SHPB. The stress in the input bar is given by the equation below (Meyers, 1994).

$$\sigma = \rho\, C_0 U_p \tag{14}$$

Equation (14) can then be used to determine the maximum impact velocity.

Since the SHPB apparatus involves the propagation of an elastic pulse through the

bars, the pulse transmitted to the input bar should have an amplitude not exceeding

the elastic limit. Using Hooke's Law, the strain in the bar is given by

$$\varepsilon = \frac{\sigma}{E} \tag{15}$$

Since we are interested in keeping the bars in the elastic region, then the maximum impact velocity U_p can be determined by

$$U_p = \frac{E\, \varepsilon_{max}}{\rho\, C_0} \tag{16}$$

where ε_{max} is $1/5\ \varepsilon_y$.

Table 1 below was developed by the researcher using materials properties by Beer et al. (2006) to serve as a guide for the maximum impact velocity for different bars and impactor materials for the SHPB test. The bar material can vary depending on the different samples or specimen material being investigated. It is important that the impact doesn't yield the bar material; if the impact velocity causes the bar material to yield then it will cause the propagation of elastic and plastic waves. Plastic waves of uniaxial stress in bars or rods are dispersive in nature and they attenuate as they propagate down the bar; if the bars remain elastic, then the pulse is propagated undistorted (Zukas et al., 1982). The stress is always much less than the elastic modulus under elastic conditions, therefore, the particle velocity U_p will be very small compared with the longitudinal wave velocity C_0 (Graff, 1991).

Table 1: Impact velocity for different bar materials for the SHPB test

Material (Beer et al., 2006)	Density (kg/m³) (Beer et al., 2006)	Elastic Modulus (Pa) (Beer et al., 2006)	longitudinal elastic wave Velocity (m/s) (Beer et al., 2006)	Yield Strength in tension (Pa) (Beer et al., 2006)	Yield Strain	Impact Velocity (m/s) $\max = \varepsilon_y$	Impact Velocity (m/s) $\varepsilon_{max} = \frac{1}{5}\varepsilon_y$
Steel							
Structural (ASTM-A36)	7860	2E+11	5044.3327	2.5E+08	0.00125	6.305416	1.2611
ASTM - A709 Grade 345	7860	2E+11	5044.3327	3.5E+08	0.001725	8.701474	1.7403
ASTM - A913 Grade 450	7860	2E+11	5044.3327	4.5E+08	0.00225	11.34975	2.2699
ASTM - A790 Grade 690	7860	2E+11	5044.3327	6.9E+08	0.00345	17.40295	3.4806
Aluminum							
Alloy 2014-T6	2800	7.5E+10	5175.4917	4E+08	0.005333333	27.60262	5.5205
Alloy 2024-T4	2800	7.3E+10	5106.0189	3.3E+08	0.004452055	22.73228	4.5465
Alloy-5456-H116	2630	7.2E+10	5232.2486	2.3E+08	0.003194444	16.71413	3.3428
Alloy-6061-T6	2710	7E+10	5082.3477	2.4E+08	0.003428571	17.42519	3.485
Alloy-7075-T6	2800	7.2E+10	5070.9255	5E+08	0.006944444	35.21476	7.043
Magnesium Alloys							
Alloy AZ80 (Forging)	1800	4.5E+10	5000	2.5E+08	0.005555556	27.77778	5.5556
Alloy AZ31 (Extrusion)	1770	4.5E+10	5042.1948	2E+08	0.004444444	22.40975	4.482
Titanium Alloy (6%Al, 4%V)	4730	1.2E+11	4930.8109	8.3E+08	0.007217391	35.58759	7.1175
Nylon, type6/6	1140	2.8E+09	1567.2078	4.5E+07	0.016071429	25.18727	5.0375
Polystyrene	1030	3.1E+09	1734.8512	5.5E+07	0.017741935	30.77962	6.1559
Vinyl, rigid PVC	1440	3.1E+09	1467.2347	4.5E+07	0.014516129	21.29857	4.2597

The selection of bars for the SHPB testing depends on a number of criteria. For example, for metals, the classical SHPB apparatus can be utilized while low impedance, low strength specimens can be tested with hollow bars. However, it is important that the length and diameter of the bar be chosen so that valid results, maximum strain rates, and strain levels are obtained. The lengths of the bars need to be chosen carefully so that they will ensure one-dimensional wave propagation for a given pulse length. For most material testing, this propagation requires the bar length to be approximately 10 bar diameters (Gray, 2000). But to readily allow separation of the incident and reflected pulse for data reduction, the bars should have length-to-diameter ratio (L/D) exceeding 20 (Gray, 2000). According to Gray (2000) the selection of the bar diameter will influence the maximum strain rate obtained from testing because the highest strain rate requires the smallest bar diameter. Another consideration for selecting the appropriate bar length is the amount of strain in the specimen that is needed by the researcher. The magnitude of the strain is related to the length of the incident pulse, requiring that the incident bar be at least twice the length of the incident pulse to prevent interference between the incident and the reflected pulses (Gray, 2000, Meyers, 1994).

Sample thickness is another important factor to be considered when testing on the SHPB system, especially on low strength, low impedance materials (Chen et al., 2000). One important requirement of the SHPB theory is that the specimen undergoes homogeneous deformation.

The SHPB experiments can also be performed at different temperatures. Researchers at Los Alamos National Laboratory have the SHPB equipment designed

to carry out experiments between -100 ^{0}F and 170^0 F (Gray and Blumenthal, 2000). Researchers have found that due to the low mechanical impedance of polymers, the signals into the pressure bars are small and sometimes non-detectable by the strain gauges affixed to them during experiments on some polymers (Gray and Blumenthal, 2000). Testing polymers at lower temperatures produces detectable signals and gives a better understanding of these polymers at high strain rate loading. With decreasing temperatures, the yield and flow stresses and yield strain increase (Siviour et al., 2005). For this reason, some tests were carried out between 0 ^{0}C and -80 ^{0}C at Los Alamos National Laboratory.

The literature for SHPB testing is immense with researchers making various modifications for testing different materials. The general principles are similar for most of the cases, and test results are valid when the correct modifications are made. Based on the literature review, some modifications have been made on the SHPB at the NMT laboratory. These modifications and the tests completed will be discussed in the following Chapters 3 and 4.

CHAPTER 3 DESCRIPTION OF THE SHPB

3.1. The Split Hopkinson Pressure Bar Apparatus in the Laboratory at New Mexico Tech

The investigation of material behavior under high strain rate has been an area of interest for engineers and researchers for the purpose of better understanding material behavior and developing constitutive equations for predicting or modeling their behavior to impact loading environments (Song and Chen, 2004). At the New Mexico Institute of Mining and Technology (NMT), student researchers are given an opportunity to investigate material behavior under high strain rate using a SHPB apparatus. This apparatus will be described briefly in this chapter and prior testing carried out by previous student researchers on the SHPB will be analyzed.

The SHPB apparatus in the NMT lab was designed and developed by the mechanical engineering students and was modified and updated by Dr. Ashok Kumar Ghosh; his contribution and enthusiasm in impact loading behavior of material made it possible for students to be able to utilize the apparatus for high strain-rate investigations. The SHPB consists of an input bar, an output bar and an impactor. An actuated ball valve releases air that is stored in a tank generated by an air compressor. The air launches the impactor causing it to strike the input bar. The strains measured by the strain gauges are recorded by a LABVIEW data acquisition system and analyzed using DIADEM analysis software.

3.2. The Components of the SHPB Apparatus

3.2.1. The Air Compressor and Reservoir

The air is supplied by a 1.8 hp, 200 psi DeWALT electric air compressor. The compressed air is released into a reservoir by relief valves. There are two relief valves; one releases the air to the reservoir and the other pressurizes the actuated ball valve for propelling the impactor. A pressure gauge measures the air pressure in the reservoir. This allows for the precise control of the reservoir pressure, on which the impact velocity is dependent. As the pressure in the reservoir is increased, the impactor velocity will be increased therefore allowing the researchers to control and vary the impact velocity for specific impactor material and length. The reservoir used in this system is a propane tank that has been modified for the SHPB apparatus. The reservoir delivers air directly to the impactor bar which is housed in a 50.8 mm pipe, projecting it towards the input bar. The pipe is fitted with an air actuated ball value at the end of the reservoir. The compressor provides air that triggers the opening of the ball valve through a circuit relay that can be activated by the researcher; the air actuated ball valve requires a pressure of 80 psi for activation and provides the best means of releasing the air from the reservoir instantaneously for launching the impactor. At the end of the impactor barrel, two light-emitting diodes (LEDs) and two SFH 314 sensors are affixed.

These LEDs and sensors provide a means of measuring the projectile/impactor velocity for different reservoir pressures. For different impactor lengths, diameters, and materials, the LEDs and sensors can be utilized to calibrate pressure against velocity. This calibration is an important aspect since it allows researchers to

investigate the relationship of impact velocity and strain rate, and also to ensure that the impactor velocity does not exceed the maximum particle velocity U_p to cause yielding in the input bar. Table 1 lists some typical bar materials and the maximum impact velocity that can be achieved on the SHPB system.

3.2.2. The Input and Output Bars

Aluminum 6061-T6 input and output bars are used for the testing of the low impedance composite material. The input and output bars are 1.2192 m long and 31.75 mm in diameter. The output bar is hollow with an internal diameter of 19.05 mm and press fitted with an aluminum end cap shown in Figure 6.

Figure 6: The end-cap fitted onto the hollow aluminum output bar

3.2.3. Instrumentation

Strain gauges are affixed at the center of the bars. The strain gauge can vary depending on the researcher's preference. For this investigation some tests were carried out using 350 ohms uniaxial strain gauges, and some carried out using 120 ohms uniaxial strain gauge depending on availability.

The strain gauges are connected to a LABVIEW data acquisition system, which records the strain readings in the input and output bars. The data analysis is done using DIADEM 8.6. This is a very powerful data analysis software and it is very practical for analyzing the data from LABVIEW. Figure 7 shows an example of the input and output graphs from the DIADEM interface, with time and strain on the x axis and y axis respectively.
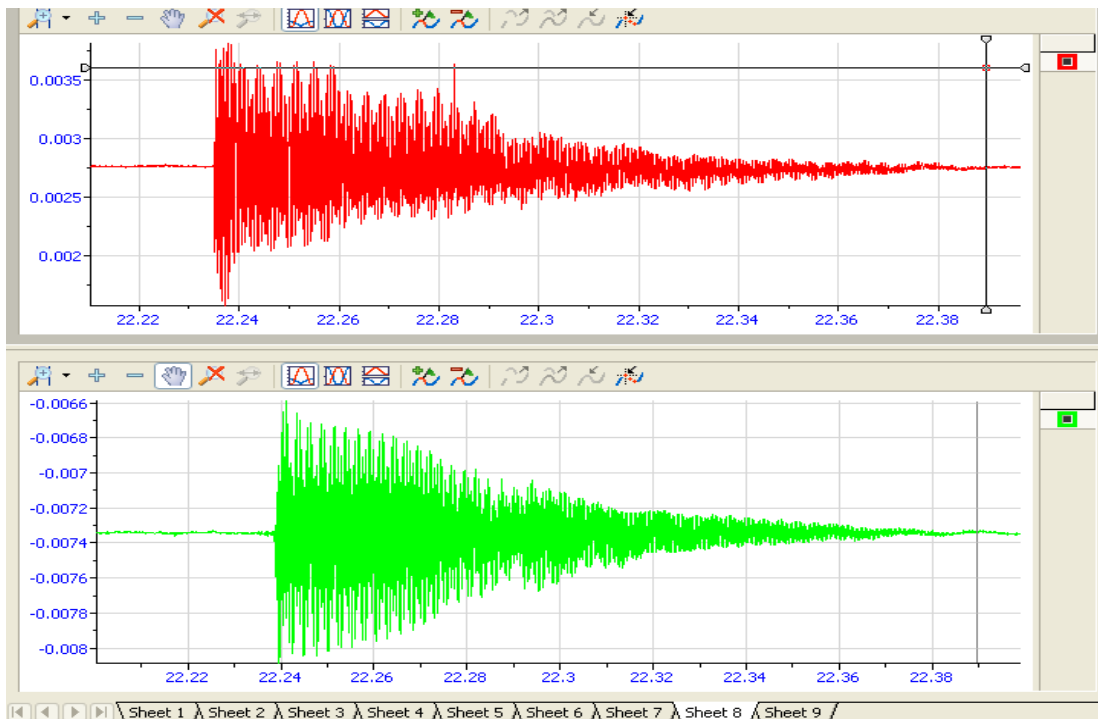
Figure 7: The input and output bar signal for testing on the SHPB

3.3. Tests Conducted by Previous Researchers

The SHPB apparatus has been used by students at the New Mexico Institute of Mining and Technology to investigate the response of materials at high strain rate loading. Jason Matthews (2008), a former graduate student at New Mexico Tech, investigated the response of polyurethane foam to impact loading using the SHPB. The result of his findings is summarized below.

Polyurethane foam is referred to as a material with low mechanical impedance and low strength (Song and Chen, 2004). Modifications are necessary to successfully utilize the SHPB apparatus for obtaining valid test data when testing soft materials. Some modifications were made by previous researchers for testing the polyurethane foam at the New Mexico Institute of Mining and Technology laboratory. These modifications include replacing the steel bars with aluminum bars; a solid input bar a hollow output aluminum bar as recommended by Chen et al. (1999). With these modifications, some tests were carried out on the polyurethane foam, some on wet samples (fluid filled) and some on dry samples. The foam samples were 12.7 mm thick.

The results obtained by Mathews (2008) reveal that the samples with water in the pores of the polyurethane foam have a higher modulus than the dry samples, and as the strain rate increased the modulus also increased. His experiments were carried out at breech pressures of 10 psi and 15 psi. These correspond to strain rates of 1088 s^{-1} and 2437 s^{-1} for dry foam and 1537 s^{-1} and 1669 s^{-1} for wet foam (Mathews, 2008). According to Mathews (2008) the dry samples have a slower strain rate at 10 psi and,

as the pressure increased, the wet samples showed a slower strain rate. At 20 psi, all

the samples exhibited signs of failure. Mathews (2008) stated that graphical

representation of the data showed that the dry samples had a lower modulus than the

wet samples at the same strain rate. The wet samples underwent less deflection than

the dry samples; they displayed 10 times the modulus of the dry samples with only

75% of the strain (Mathews, 2008). The fluid in the foam is pushed into empty pores

upon impact and thereby absorbing the impact energy more effectively than the foam

alone. Table 2 below is a summary of Mathews's work on the SHPB with the wet and

dry foam samples (Mathews, 2008).

Table 2: High Strain rate data for wet and dry polyurethane foam (Mathews, 2008)

Test #	Sample Condition	Modulus (MPa)	Strain Rate (s^{-1})	Tank Pressure
1	dry	2.25	1088	10
2	dry	2.53	1101	10
3	dry	2.33	1078	10
4	dry	2.84	1086	10
5	dry	2.13	1088	10
6	wet	132	1538	10
7	wet	130	1523	10
8	wet	128	1532	10
9	wet	134	1567	10
10	wet	133	1525	10
11	dry	21.3	2341	15
12	dry	148	1687	20
13	dry	20.9	2461	15
14	dry	22.6	2511	15
15	dry	19.8	2437	15
16	wet	332	1687	15
17	wet	583	1937	20
18	wet	327	1701	15
19	wet	341	1665	15
20	wet	311	1623	15

The preliminary data for the foam samples obtained by Mathews (2008) as shown in Table 2 above was plotted in Figure 8. It shows a dramatic increase in the modulus of the fluid filled samples compared to the increase in the modulus of the dry samples. Figure 9 compared the data of foam samples obtained by Mathews (2008) and the author. "JM" represents Mathews's data and "NB" represents the author's data. The difference between these sets of data is noticeable.

Two factors that may have contributed to these differences are sample size and temperature of testing. Mathews (2008) placed the foam specimen in a sample holder between the input and out bars, with the specimen larger than the bar diameter. The author however, sandwiched specimen of 25.4 mm diameter directly between the input and output bars. According to Gray (2000) specimen should be 80% of the bar diameter to allow for 30% strain before the specimen exceeds the bar diameter. The temperature of testing environment may also be a contributing factor. According to Siviour et al. (2005) the mechanical properties of polymers are effect by temperature. Since the testing was done in a warehouse at different seasons, temperature could have influenced the results.

Most of Mathews (2008) experiments were carried out under blast loading at EMRTC. He subjected the foam samples to explosive charge and recorded their behavior. The reader is encouraged to review his work for an in-depth discussion of the foam's behavior under blast loading.
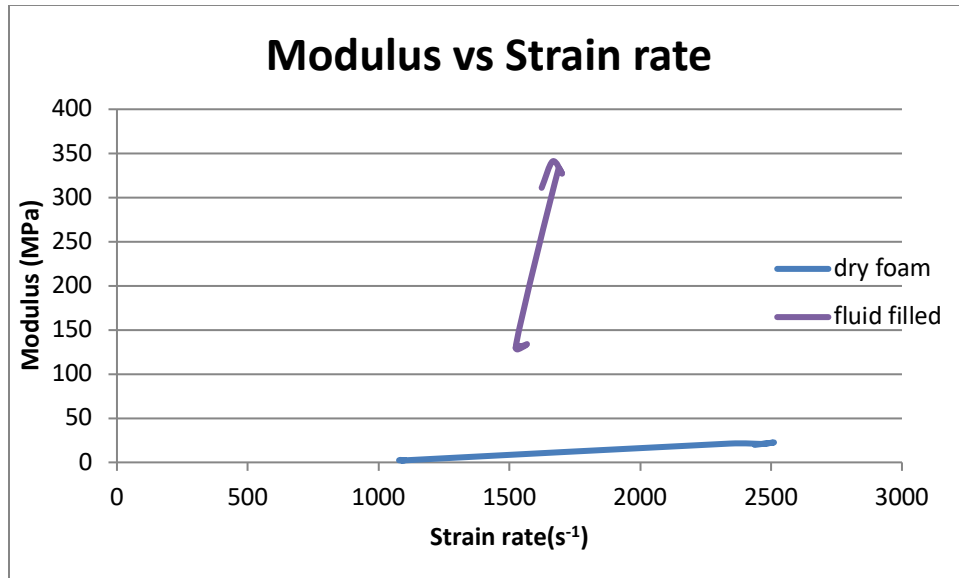
Figure 8: The effect of strain rate on modulus (Mathews, 2008)
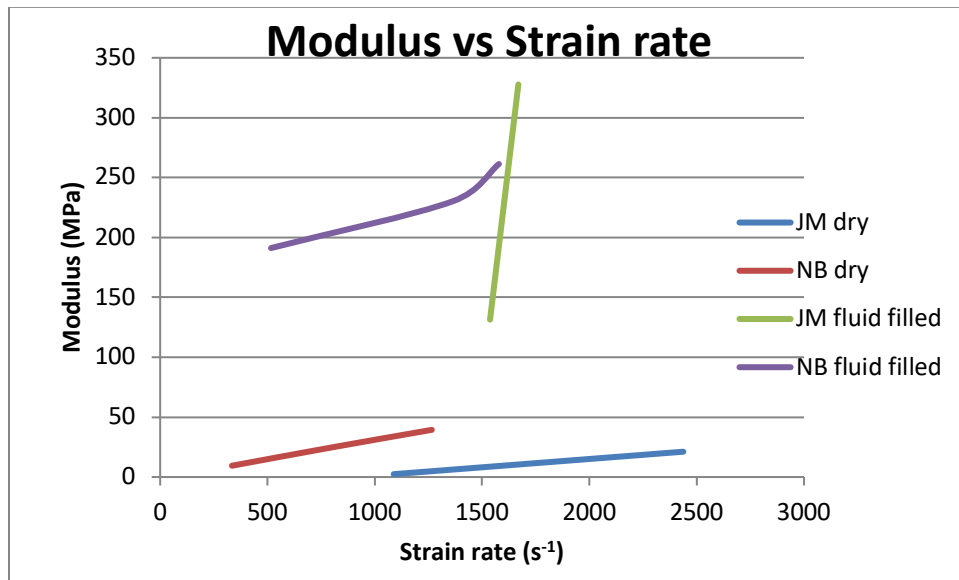
Figure 9: Comparison of previous (Mathews, 2008) and current (researcher) results of strain rate on modulus

31

These preliminary results seem promising and therefore further investigations were carried out with the same polyurethane foam. However, the foam was sandwiched by Kevlar skin layers and subjected to impact loading. Kevlar was selected after an intense literature review for a suitable skin layer. Many different fabrics that were thoroughly researched for the skin layers include carbon fiber, Kevlar, Nomex, fiberglass, and ballistic nylon (Ghosh et al. 2010). Kevlar find applications in bulletproof vests, puncture resistant vests, needle resistant gloves, helmets, and kayaks. There are different grades of Kevlar such as Kevlar 29, 49, and 149 with the greater number indicating a higher tensile modulus, but a lower tensile elongation. Generally, this fabric is very strong for its weight with a high modulus and high flexibility. It is also fire resistant and will not combust, but only degrade at high temperatures (800° to 900°F) (Ghosh et al. 2010).

3.4. Sample Preparation

For reliable data, care must be taken in preparing samples for testing on the SHPB apparatus. There are some basic requirements that must be met for samples that are to be tested on the SHPB apparatus. These include:

1. The faces of the samples must be flat so that excellent contact can be established with the pressure bars and the sides must be orthogonal to the loading surface for uniform elastic loading (Gray, 2000).

2. When preparing samples for testing on the SHPB, the thickness is the dominant factor for consideration for a given sample diameter because it affects the

dynamic stress equilibrium process; a fundamental requirement of the SHPB analysis (Song and Chen, 2004, Gray, 2000). These requirements were considered and satisfied while preparing samples for this investigation. Precaution was taken during the manufacturing of the composite samples for testing to ensure that all samples were made appropriately.

The composite material was prepared using polyurethane foam and Kevlar. The foam and Kevlar were bonded with MAS epoxy resin and hardener to produce a sandwiched composite material with the foam on the inside. The figure below is an example of the sandwich polyurethane foam composite.
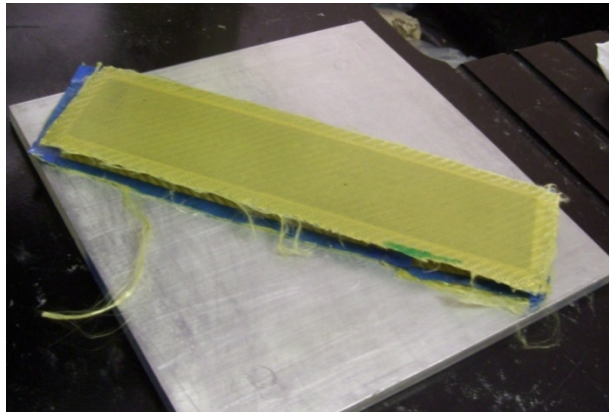
Figure 10: Sandwich composite of polyurethane foam and Kevlar

Tests were also carried out on samples which had the pores of the foam filled with fluid (wet samples). Filling the foam with fluid was done after the composite materials had been constructed. As discussed earlier, test results obtained by Mathews (2008) revealed that fluid in the pores of the polyurethane foam produced a

material with promising shock absorbing properties. Modifications to rectify some of the deficiencies of axial alignment and reliable pressure measurements with the previous SHPB apparatus were made and additional experiments were conducted to further investigate this material's behavior to impact loading.

3.5. Modifications of the SHPB for Current Testing

Some of these modifications include affixing a pressure gauge to the reservoir to more precisely measure the tank pressure and create a more user friendly operating system. Previously, the reservoir pressure was measured using a pressure transducer that required the usage of a voltmeter to measure voltage and correlate the readings to pressure. This was a time consuming process which created the introduction of human error; with the dial pressure gauge, measurements were quick and accurate.

To further increase the alignment of the pressure bars, additional supports were installed onto the system. According to Zukas et al., (1982) precise alignment of the pressure bars is crucial. Additional supports made of aluminum and Teflon bushings were installed to allow the stress wave to pass without dispersion. Some fine adjustments were made to further align the bars precisely (optimal axial alignment), these include readjusting the existing supports which were found to be slightly misaligned and cleaning of the barrel to allow the impactor to travel unimpeded towards the input bar. Also, the input and output bars were sanded so that they are smoother and can move without restraint; one important requirement according to Gray (2000). A new end cap was also made and fitted onto the hollow output bar. When using a hollow output bar, the end cap should be press fitted onto the end of the

34

bar, it should fit firmly (Chen et al., 1999). The old cap was fitted snugly which could be a source of error.

The completed modifications made the system more efficient and testing could be conducted. The experiments were conducted between 5 psi and 15 psi tank pressure range. The testing procedure will be discussed in Chapter 4.

CHAPTER 4 TESTS CONDUCTED

4.1. Test Matrix

Many different samples were made according to the test matrix shown in Table 3 below and were tested under the standard test procedure of the SHPB apparatus at various breech pressures. The preparation of the different samples and sample testing are discussed in this chapter.

Table 3: The test matrix

Impact pressure (psi)	Sample description
5	
10	A, B, C, D
15	

Sample description:

A: foam only

B: foam + 779 Kevlar (one face only)

C: foam + 779 Kevlar (both faces)

D: foam + 2 x3 Kevlar on both faces

The total mass of a 101.6 mm square sample with one layer of Kevlar on both sides is approximately 45 grams. The mass of each component is as follows:

Mass of 101.6 mm square 2x3 Kevlar = 3.73 g

Mass of 101.6 mm square fine weave Kevlar = 1. 38 g

Mass of 101.6 mm square polyurethane foam = 31.69 g

Mass of MAS epoxy resin and hardener for 101.6 mm square sample = 7.5 g

The foam material used is open cell quick recovery polyurethane foam of 25.4

diameter and 12.7 mm thickness. The density of the foam material is 15 lb/ft^3 and its

tensile strength of 40 psi (Rogers Corporation, 2010)

The composite samples were prepared according to the matrix in Table 3. The

basic materials used were quick-recovery polyurethane foam, Kevlar fibers, and

epoxy-resin. A detailed explanation of the composite sample preparation will not be

discussed because it involves patented information. The different samples prepared

are shown in Figure 11 below.
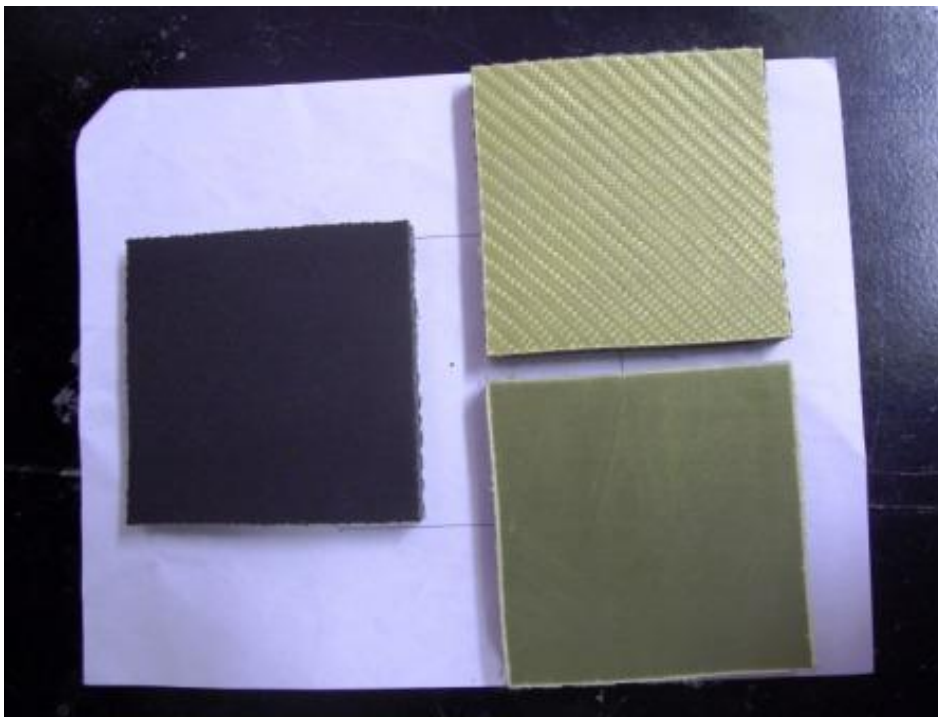
Figure 11: The different samples prepared for testing

4.2. Test Procedure

1. The different composite samples were prepared.

2. Foam samples were cut to the required size using a coring tool. The composite samples were cut using a band saw. After the samples were cut to the desired dimension they were tested under impact loading.

3. For testing, the sample was sandwiched between the bars and a small amount of vacuum grease was applied to the sample ends of the input and output bars to keep the sample in position and avoid any effects of friction, according to Chen et al. (2000) petroleum jelly is also effective.

4. The striker bar (impactor) was pushed back into the barrel towards the actuated ball valve on the reservoir so that upon the opening of the valve, the air pressure will propel the striker bar forward and produce the impact on the input bar.

5. The air compressor was used to pressurize the reservoir to the desired pressure for the different impact velocities.

6. After pressurizing the reservoir, LabView VI was opened.

7. The actuated ball valve connected to the reservoir was activated and the projectile launched, producing an impact in the input bar, which propagated through the sample and the output bar.

8. The strain gauges on the input and output bars were used to record the strain caused by the impact and the data was analyzed.

Steps 2 – 7 were repeated for all the different samples to generate the data needed for this report. Tests were also carried out at Los Alamos National Laboratory and these data were compared to those obtained in the lab at NMT.

4.3. Experiments Conducted at LANL

Experiments were also conducted at Los Alamos National Laboratory on the SHPB apparatus at temperatures between 0^0C and -80^0C using solid magnesium pressure bars of 9.525 mm diameter. The input and output bars were 762 mm long while the striker bar was 152.4 mm long. Figure 12 shows the SHPB at Los Alamos National Laboratory. The researchers at Los Alamos National Laboratory can conduct experiments on their SHPB apparatus over a range of temperatures.

Figure 12: The SHPB apparatus at LANL (Courtesy of C. M. Cady)

Researchers at LANL are conducting high strain rate testing on materials between -100 and 170^0 F (Gray et al., 2000). The samples can be cooled or heated depending on the testing data desired. According to Gray et al. (2000) cooling and heating of samples is done by Helium gas within a stainless steel containment chamber at partial vacuum. By passing helium through a copper coil positioned within liquid nitrogen dewar, cooling of the helium gas below ambient temperature is

obtained; while heating the helium in a parallel coil within a glycerin-filled beaker warmed by a heating plate produce heated samples (Gray et al. 2000). Figure 13 shows the heating and cooling setup for controlled temperature testing on the SHPB apparatus at Los Alamos National Laboratory. A thermocouple positioned to lightly touch the outside of the sample is used to monitor the temperature of the sample. The flow rate of the helium gas around the manifolds can be controlled to adjust/regulate the temperature of the sample (Gray et al., 2000).
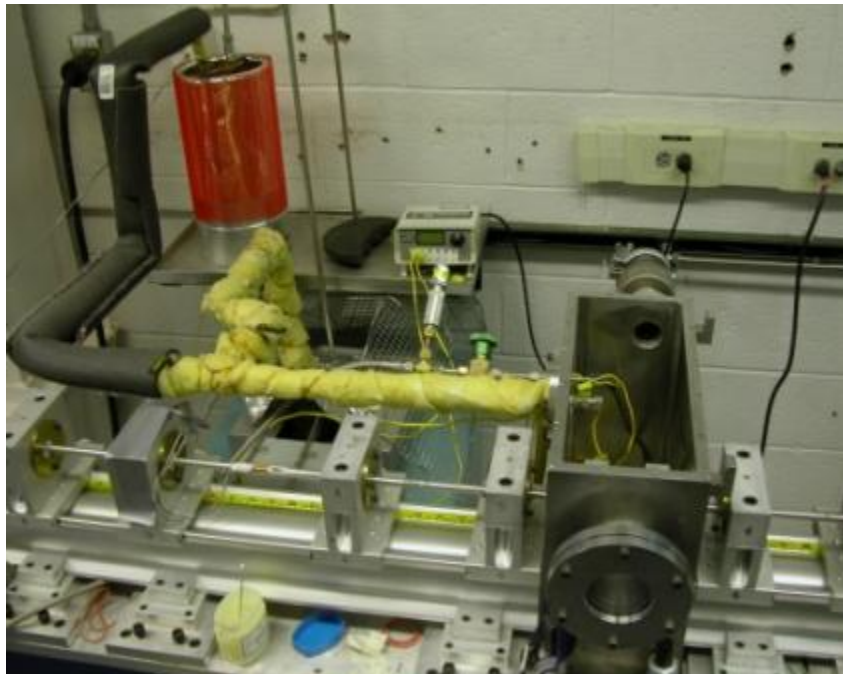
Figure 13: The heating or cooling setup for controlled temperature testing (Courtesy of C. M. Cady)

The advantage of testing at lower temperature (below 77^0 F) for a range of polymers show that both the measured loading elastic modulus and the measured peak flow stress increases with decrease temperature (Kukureka and Hutchings, 1984, Walley et al., 1991). Also, the behavior of polymers and polymer composites for

temperatures between -40 ^{0}C and 40 ^{0}C are relevant for arctic to desert environments (Gray et al., 2000).

Polyurethane foam samples were tested between 0 ^{0}C and -80 ^{0}C at Los Alamos National Laboratory. The samples were 7.9375 mm in diameter and 4.7625 mm in length. The data obtained from these tests are used to formulate a simple relationship between strain rate and modulus for the polyurethane foam that has been used as the core layer for the composite material.

CHAPTER 5 RESULTS AND DISCUSSION

Modifications were made to the conventional SHPB to investigate the impact response of a composite material consisting of polyurethane foam and Kevlar. The steel bars of the SHPB apparatus were replaced with aluminum rods to cater to the impedance mismatch of the very low mechanical impedance foam material. A hollow aluminum tube was used for the output bar to produce a magnified signal of the transmitted pulse. According to many researchers, the low impedance material causes most of the incident pulse to be reflected back into the incident bar, resulting in a very low transmitted signal through the specimen (Chen et al., 1999). Test results of the composite material confirm this observation. During the analysis of the strain measurement from the input and output bars, the difference between the strain measurements (signal amplitude) was considerable.

5.1. Tests Completed at NMT Laboratory

The foam and different composite samples were tested on the SHPB apparatus. Tables 4 – 9 show the values of stress, strain and strain rate obtained from the experiments. These results show that with increasing velocities, the stresses, strains and the strain rates increased. The stress and strain values were used to determine the average dynamic modulus of the foam and composites. As expected, the dynamic modulus of the foam and composite samples increased with increasing strain rate. Also, the fluid filled composites exhibited an increase in dynamic modulus when compared to the dry samples.

Table 4: Mechanical properties of foam sample

Stress σ_s (MPa)	Strain ε_s	Strain rate $\acute{\varepsilon}_s$ (s^{-1})	Modulus (MPa)	Impact Vel. (m/s)
10.75393	0.05395	537.6173	199.3331	10.7
10.38436	0.048235	495.2771	215.2876	10.7
26.05064	0.13312	1416.569	195.6926	15.8
26.43303	0.13597	1356.6	194.4041	15.8
24.31467	0.130893	1322.281	185.7599	15.8
30.96925	0.133597	1328.457	231.8106	19.8
41.67875	0.143285	1433.401	290.8795	19.8

Table 5: Mechanical properties of foam + 1 side fine weave Kevlar

Stress σ_s (MPa)	Strain ε_s	Strain Rate $\acute{\varepsilon}_s$ (s^{-1})	Modulus (MPa)	Impact Vel. (m/s)
9.647455	0.101541	1014.973	95.01058	10.7
11.10345	0.10207	1032.915	108.7826	10.7
18.77432	0.113477	1140.833	165.4468	15.8
13.40576	0.119542	779.7041	112.1424	15.8
20.04733	0.18639	1839.758	107.5557	19.8
21.64255	0.157143	1562.798	137.7248	19.8

Table 6: Mechanical properties of foam + fine weave Kevlar on both sides

Stress σ_s (MPa)	Strain ε_s	Strain rate $\acute{\varepsilon}_s$ (s^{-1})	Modulus (MPa)	Impact Vel. (m/s)
1.763975	0.064577	358.8964	27.31584	10.7
2.789896	0.034899	226.7614	79.94282	10.7
14.19881	0.084288	418.4153	168.4558	15.8
17.80375	0.086368	689.1492	206.1375	15.8
23.64478	0.099043	977.6156	238.733	19.8
33.61758	0.164117	1210.659	204.8393	19.8

Table 7: Mechanical properties of foam + 2x3 Kevlar on both sides

Stress σ_s (MPa)	Strain ε_s	Strain rate $\acute{\varepsilon}_s$ (s$^-$)	Modulus (MPa)	Impact Vel. (m/s)
0.467077	0.074601	445.1238	6.26102	10.7
0.369439	0.066333	375.4984	5.569474	10.7
0.636555	0.063994	364.8584	9.947137	10.7
0.738918	0.055115	549.2929	13.4068	15.8
0.936947	0.082989	571.6087	11.28997	15.8
1.255223	0.091433	922.5778	13.72838	19.8
1.404918	0.097226	959.3573	14.44997	19.8
1.67882	0.089524	917.7211	18.75279	19.8

Table 8: Mechanical properties of fluid-filled foam + 2x3 Kevlar on both sides

Stress σ_s (MPa)	Strain ε_s	Strain rate $\acute{\varepsilon}_s$ (s^{-1})	Modulus (MPa)	Impact Vel. (m/s)
1.138536	0.031659	158.1064	35.96268	10.7
2.625775	0.056414	388.5866	46.5446	10.7
1.883701	0.050057	492.6979	37.63125	10.7
5.203985	0.083646	547.8092	62.21467	15.8
3.905243	0.059806	605.0019	65.29846	15.8
3.78235	0.070272	592.963	53.82449	15.8
6.869903	0.094839	951.5612	72.43789	19.8
9.740882	0.121893	797.3087	79.91326	19.8

Table 9: Mechanical properties of fluid-filled foam + fine weave Kevlar on both sides

Stress σ_s (MPa)	Strain ε_s	Strain rate $\acute{\varepsilon}_s$ (s^{-1})	Modulus (MPa)	Impact Vel. (m/s)
1.598833	0.05481	482.6347	29.17072	10.7
1.961753	0.040292	218.2006	48.68851	10.7
2.675927	0.076283	523.3456	35.0789	10.7
2.700793	0.070979	699.1439	38.05033	15.8
3.025265	0.084337	665.6543	35.87118	15.8
3.719776	0.09971	685.4099	37.30601	15.8
8.801644	0.094614	929.9557	93.02682	19.8
7.566241	0.093318	922.551	81.08005	19.8

An aluminum specimen was tested on the SHPB to verify that the low impedance material was responsible for most of the incident wave to be reflected back into the input bar. In fact, the results of the aluminum testing show that most of the incident pulse was transmitted through the sample and registered in the output bar. As mentioned previously, the stress in the sample is a function of the transmitted

pulse (Equation (9)); testing verified that increasing the impact load on the aluminum sample produced greater stress. The mechanical properties of the aluminum sample are shown in Table 10 below.

The test results of the composite material and foam samples were similar to each other because, in both cases, most of the incident pulse was reflected back into the input bar which is an indication of the amount of strain and strain rate in the sample (Equations (8) and (10)). The test results disclose that the foam and composite samples experienced a higher strain and strain rate than the aluminum because of the greater reflected pulse in the foam and composite samples.

The composites were then tested with fluid in the pores of the foam (wet samples).The results of the wet samples (Table 9) show that they experienced lower strain values than the dry composite samples. The strain values of the wet samples can be compared to the aluminum sample, but the modulus values were different.

Table 10: Mechanical properties of 6061-T6 Aluminum

Stress σ_s (MPa)	Strain ε_s	Strain rate $\acute{\varepsilon}_s$ (s^{-1})	Modulus (MPa)	Impact Vel. (m/s)
50.03115	0.013513	153.8843	3702.338	10.7
52.58797	0.024376	240.3437	2157.371	10.7
51.07578	0.02142	213.5514	2384.488	10.7
58.99373	0.027729	275.3403	2127.486	15.8
62.90467	0.030675	301.3191	2050.664	15.8
61.49126	0.036754	367.2329	1673.037	15.8
72.52011	0.039819	392.4277	1821.255	19.8
77.15915	0.042889	430.169	1799.034	19.8
91.24592	0.071723	355.8085	1272.191	19.8

Figure 14 shows the stress vs. strain rate graphs for the different samples tested. The graphs reveal an increase in stress as the strain rate was increased for the different specimen. Figure 15 shows the modulus vs. strain rate. It can be seen that the aluminum sample exhibited a decrease in modulus as the strain rate was increased while the other composite samples confirm an increased in modulus with increasing strain rate.
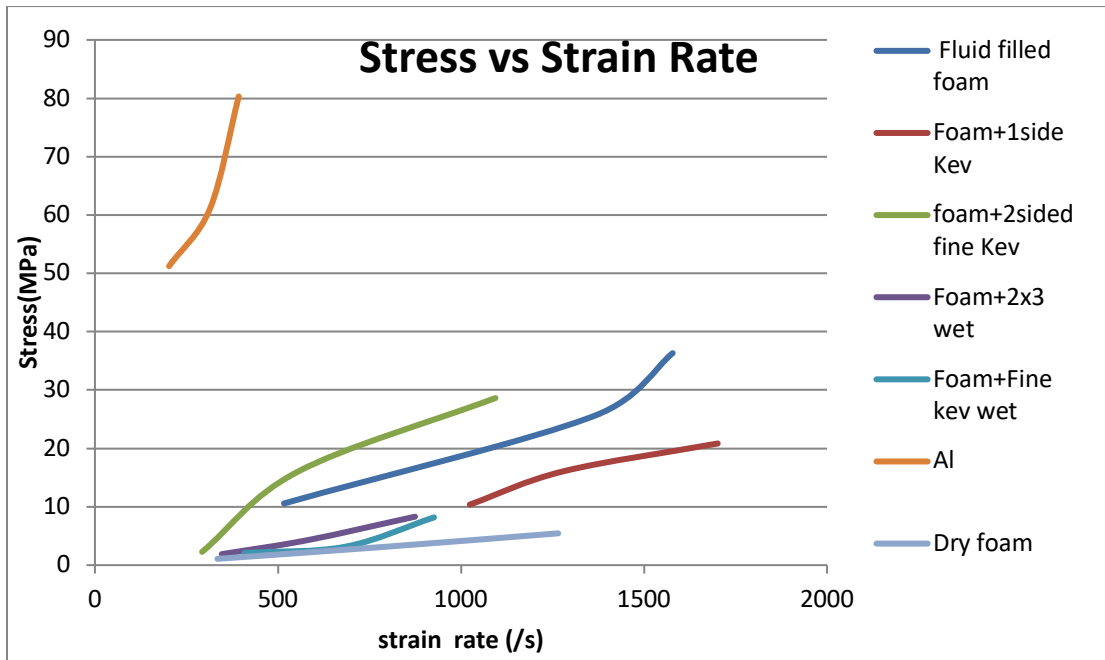
Figure 14: Stress vs. Strain rate for different samples

Modulus (MPa) vs Strain Rate
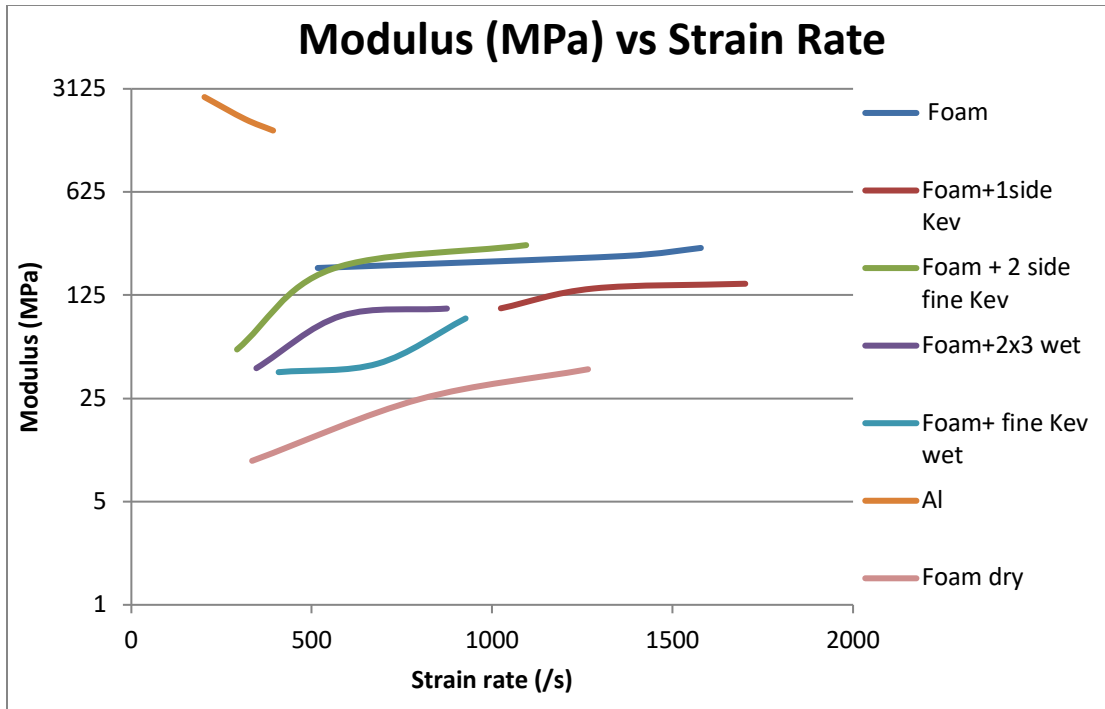
Figure 15: Modulus vs. Strain rate for the different sample tested

According to Zukas et al. (1982), this increase in stiffness is due to the increase in the cross-sectional area of the specimen. The sample strains upon impact and expands, increasing its surface area to the load. Because the aluminum sample is made of a material with a higher modulus of elasticity, it will not experience as large a change in cross-section as the polyurethane foam. Also, the material work-hardens as deformation proceeds, making it stiffer as strain increases (Zukas et al., 1982). This explains the increase in the modulus of the foam and composite specimens as the strain rate or impact velocity increases between the ranges of 100 $^{s-1}$ to 1500 s^{-1}.

5.2. Results of Foam Samples from LANL

The following Table 11 gives the properties of the SHPB apparatus at Los Alamos National Laboratory. The testing was done on the SHPB with 9.525 mm

diameter magnesium bars. The researchers at Los Alamos National Laboratory use solid bars with very small diameter to achieve a higher strain rate.

Table 11: The properties of the SHPB material at LANL

Breech Pressure(psi)	5.0
Striker Length(mm)	152.4
Incident Bar Young's Modulus(GPa)	42.957893
Incident Bar Poisson Ratio	0.310749
Incident Bar Rod Sound Speed(m/s)	4913.981418
Incident Bar Longitudinal Sound Speed(m/s)	5792
Incident Bar Shear Sound Speed(m/s)	3035
Incident Bar Density(kg/m^3)	1.779
Transmitted Bar Young's Modulus(GPa)	42.957893
Transmitted Bar Poisson Ratio	0.310749
Transmitted Bar Rod Sound Speed(m/s)	4913.981418
Transmitted Bar Longitudinal Sound Speed(m/s)	5792
Transmitted Bar Shear Sound Speed(m/s)	3035
Transmitted Bar Density(kg/m^3)	1.779

The stress strain graph shown in Figure 16 was obtained after testing the polyurethane foam at three different pressures at room temperature. The sample was 7.9375 mm in diameter and 4.7325 mm thick. Due to the soft nature of the specimen, the transmitted signal detected by the strain gauge on the solid output bar was unreliable to be used for any analysis. It was then decided to increase the breech pressure for a higher impact velocity and better transmitted signal into the pressure bars. This did not noticeably improve the results and the breech pressure could not be increased further because higher impact velocity could yield the pressure bars. After analyzing these results, it was decided to test the samples at lower temperature. The results at different temperatures are discussed below. Figure 17 shows the average strain rate vs. average strain for temperatures between 0^0C to -60^0C. It demonstrated the constant strain rate required for SHPB testing (Gray, 2000). Figures 18 - 25 display the results of the foam material tested at temperatures between 0^0C and -80^0C.
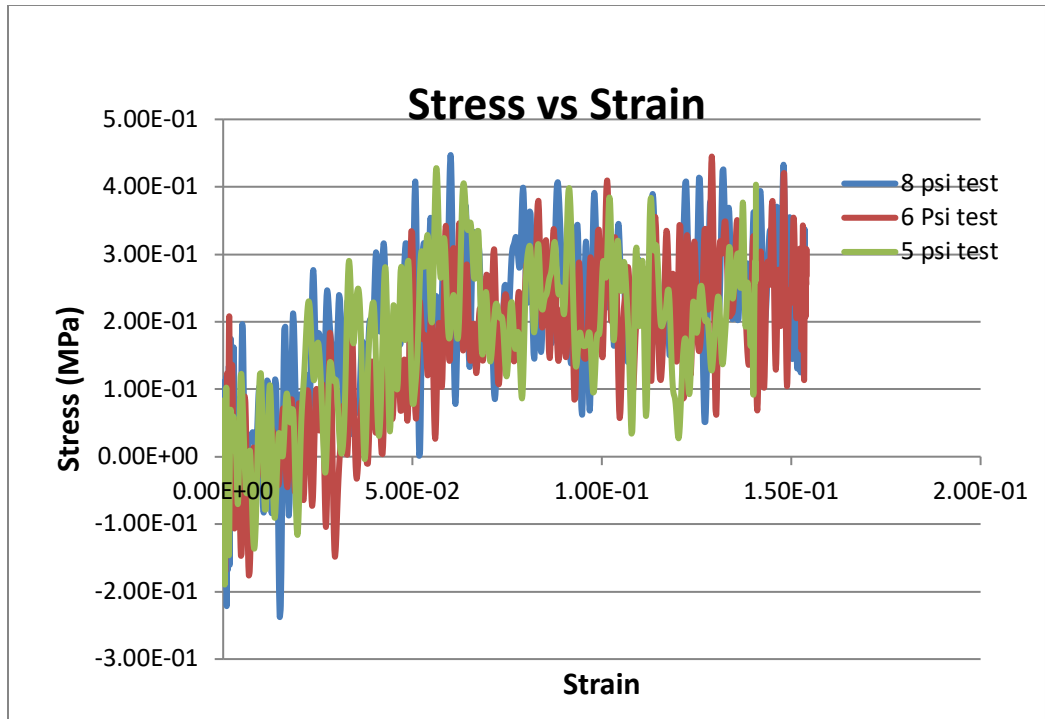
Figure 16: The stress-strain graph of polyurethane foam at room temperature
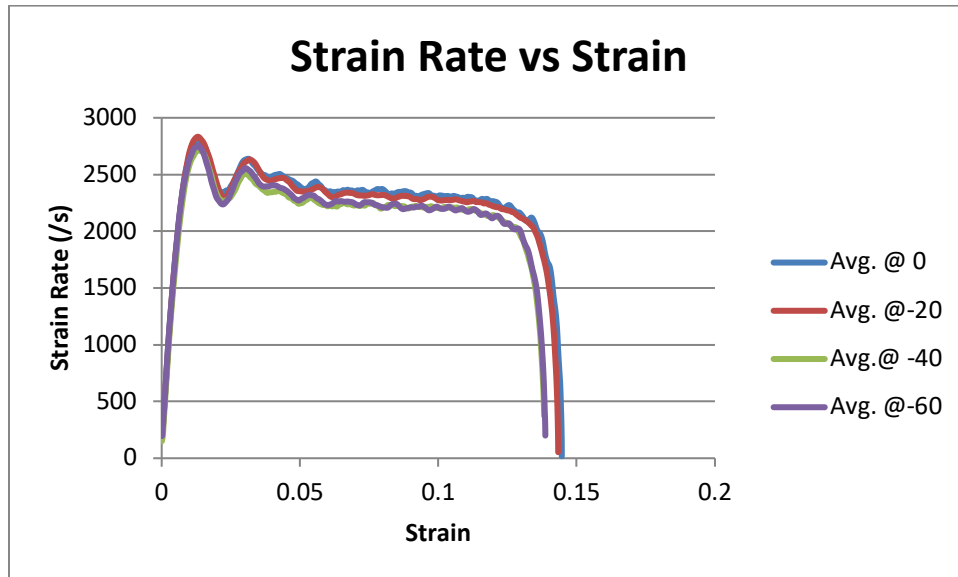
Figure 17: Strain rate vs. strain at different temperature
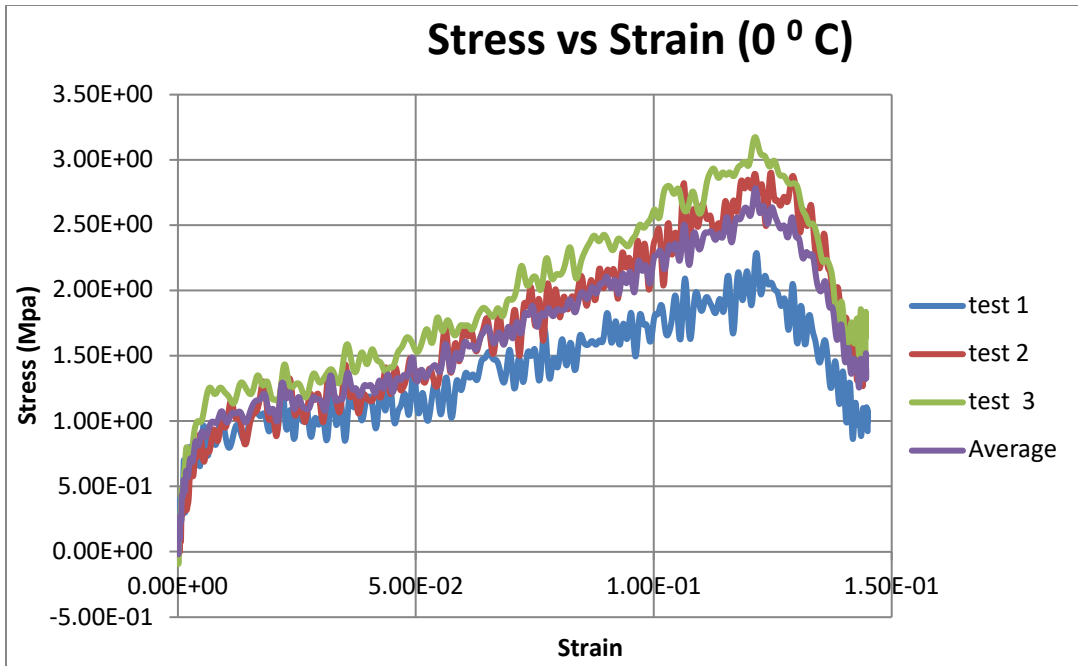
Figure 18: The stress-strain graph of polyurethane foam at 0^0 C
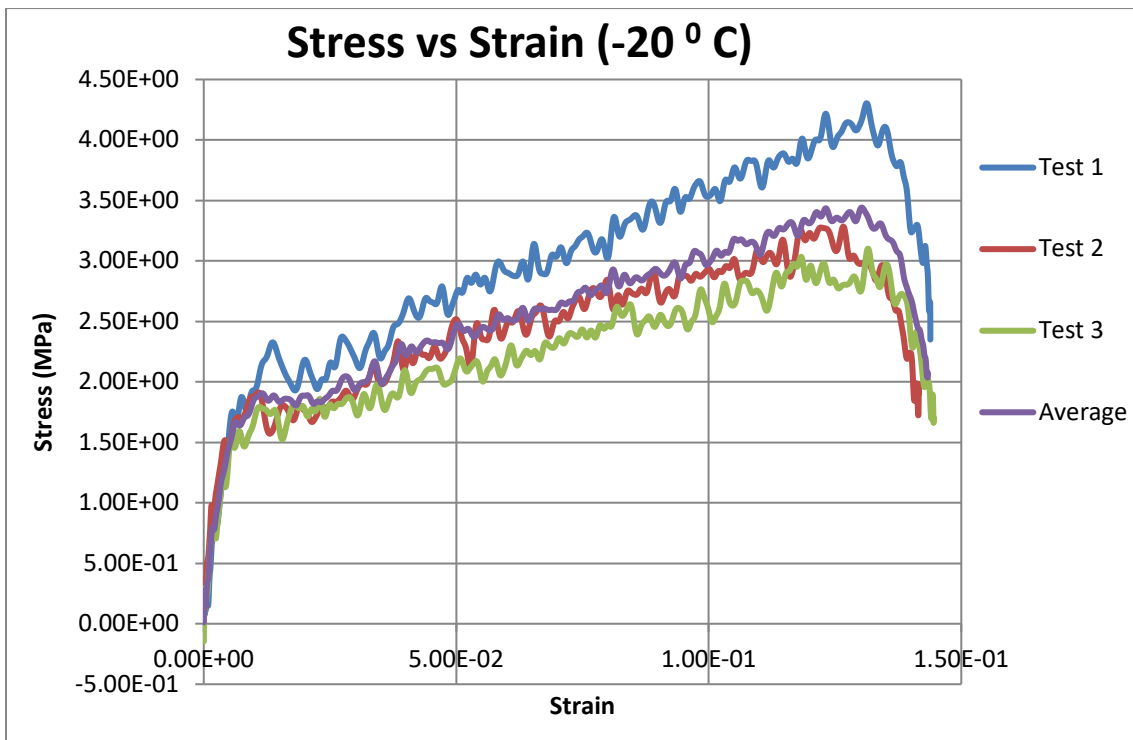
Figure 19: The stress-strain graph of polyurethane foam at -20^0 C
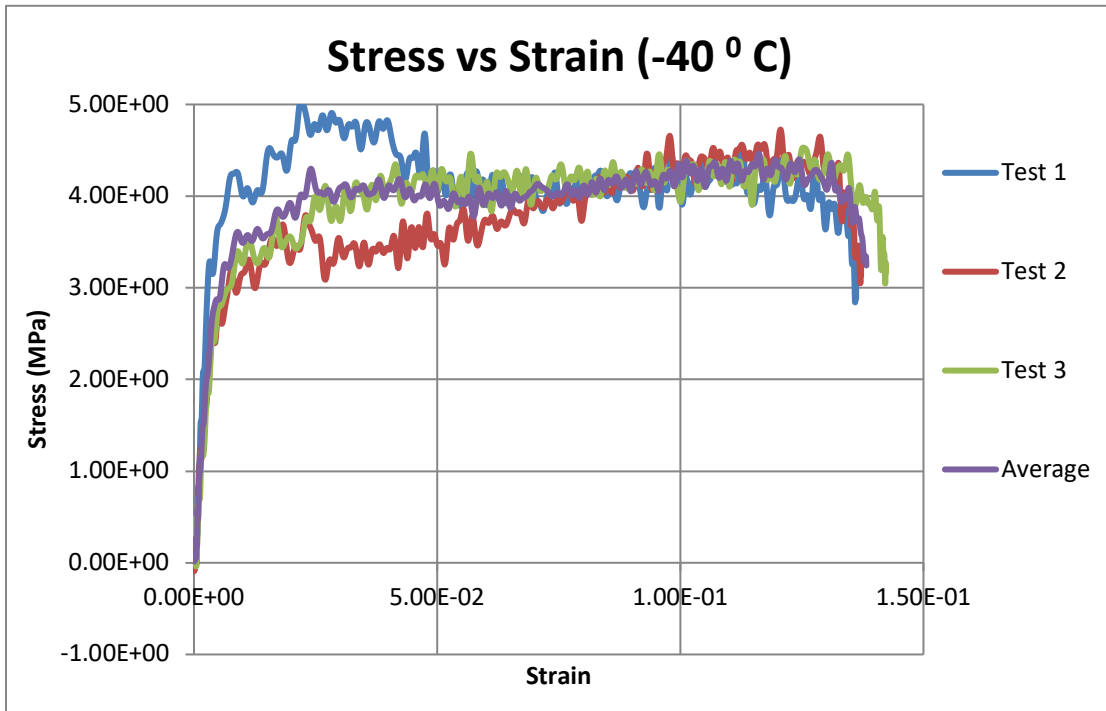
Figure 20: The stress-strain graph of polyurethane foam at -40^0 C
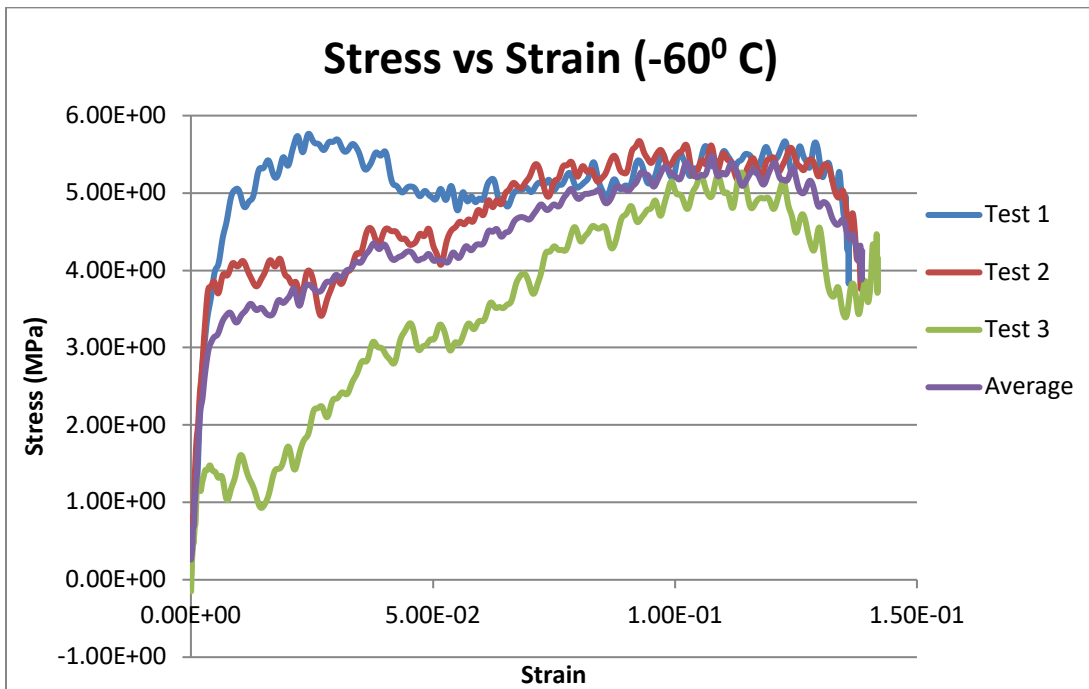
Figure 21: The stress-strain graph of polyurethane foam at -60^0 C
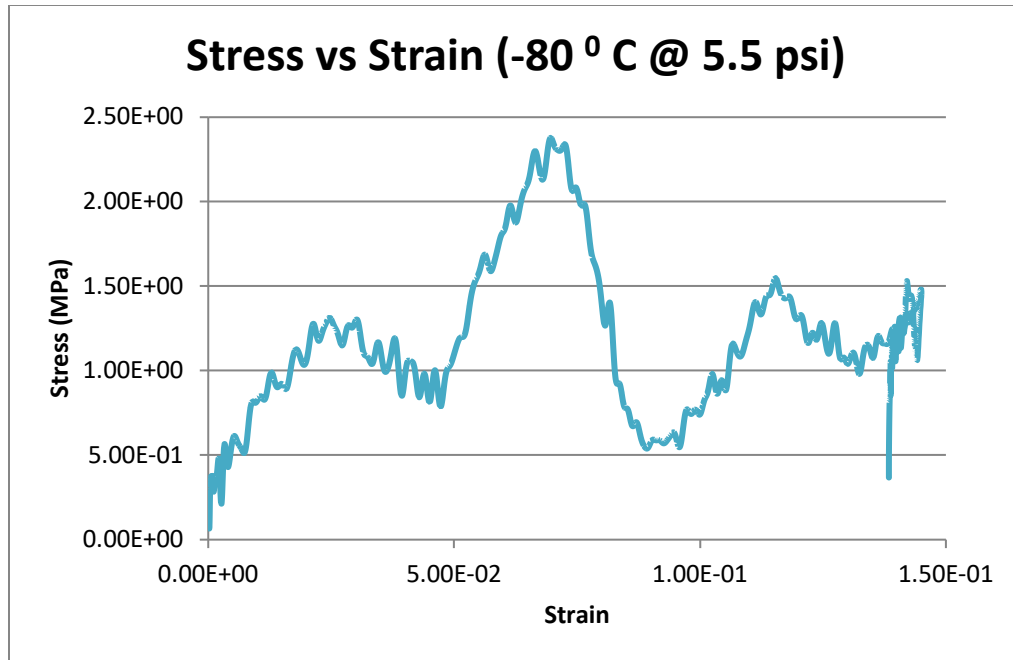
Figure 22: The stress-strain graph of polyurethane foam at -80^0 C
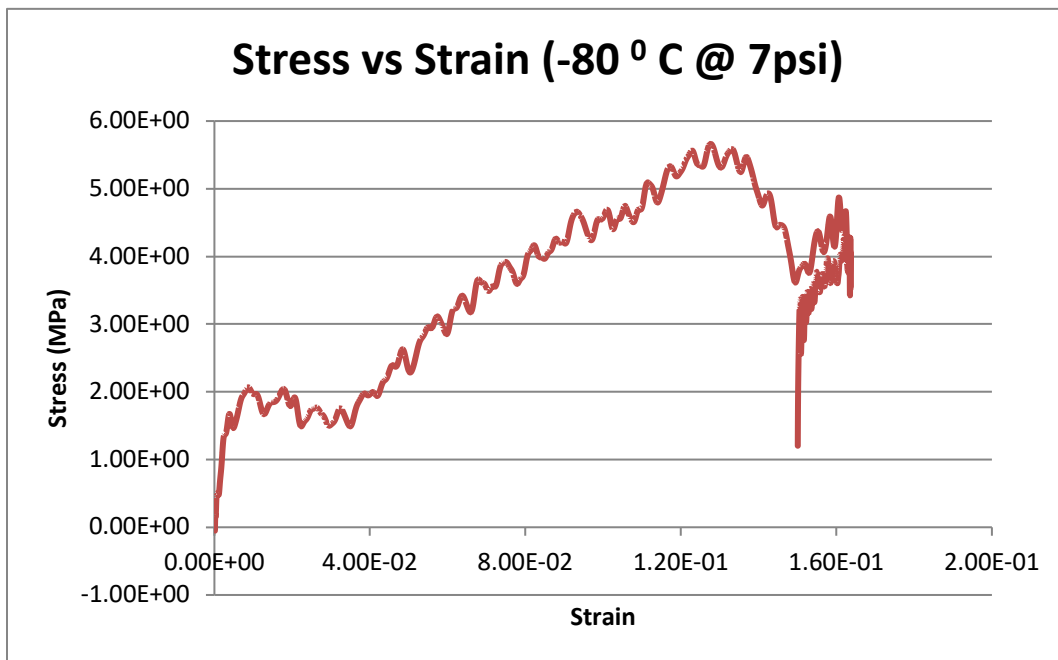
Figure 23: The stress-strain graph of polyurethane foam at -80^0 C
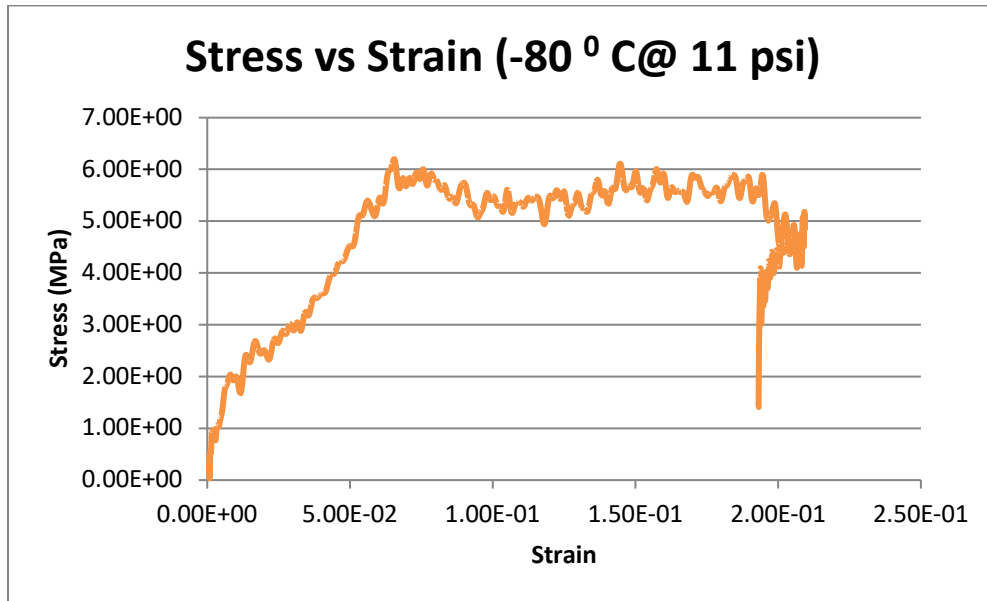
Figure 24: The stress-strain graph of polyurethane foam at -80^0 C
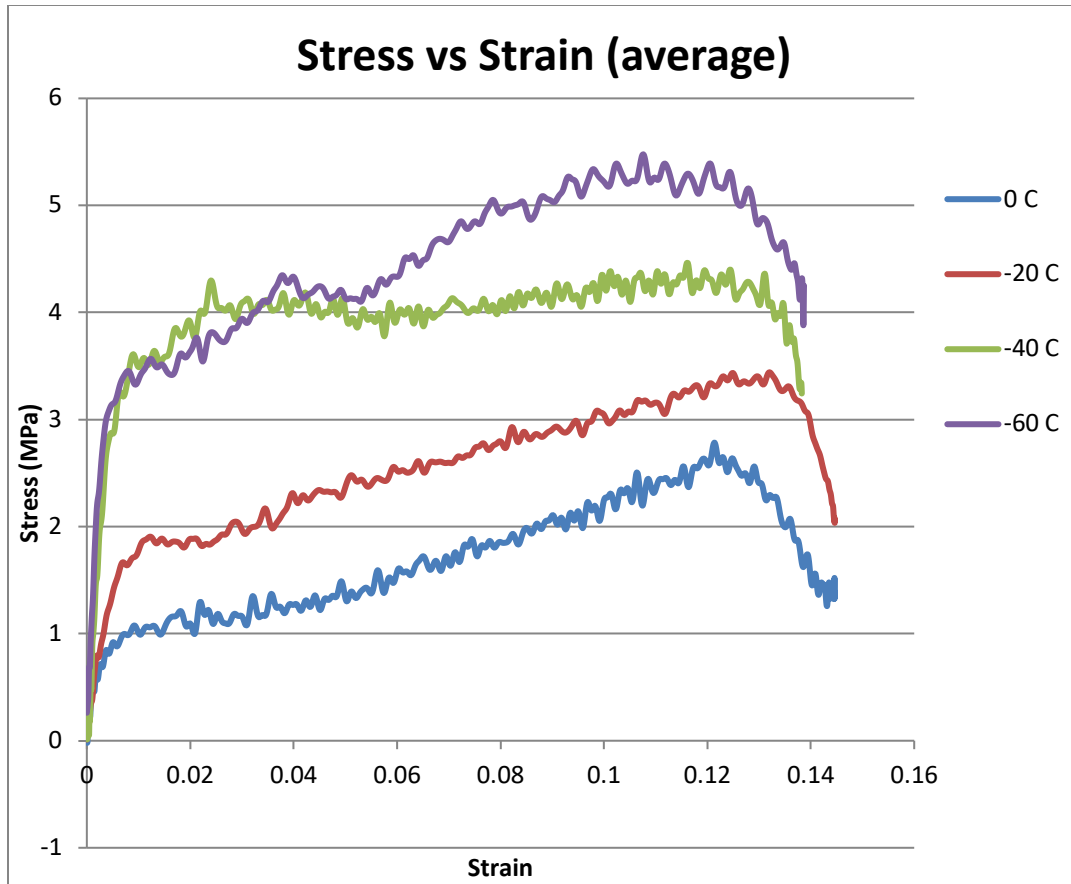
Figure 25: Stress-strain graph of polyurethane foam at different temperatures

According to the Siviour et al. (2005) yield and flow stress for some polymers increase with decreasing temperature; Figure 26 shows the stress vs. temperature for the foam specimen and the increase in yield stress with decreasing temperature is evident. Using the data obtained from the low temperature experiments Figures 27 and 28 were developed to deduce a relationship between modulus and strain rate. Figure 25 yield Equation (17) with modulus as a function of temperature.

$$y = -0.5839x + 16.906 \tag{17}$$

Figure 26 yield Equation (18) with strain rate as a function of temperature

$$y = -1.3167x + 1508 \tag{18}$$

By solving Equation (18) for strain rate and substituting into Equation (17) a simple linear equation was developed with modulus as a function of strain rate after adjusting for initial condition of zero strain rates at room temperature and assuming that the trend of decreasing modulus with increasing temperature continues to room temperature.

$$M = 0.4435\acute{\varepsilon} + 2.3 \qquad (19)$$

Where M is the modulus and $\acute{\varepsilon}$ is the strain rate.
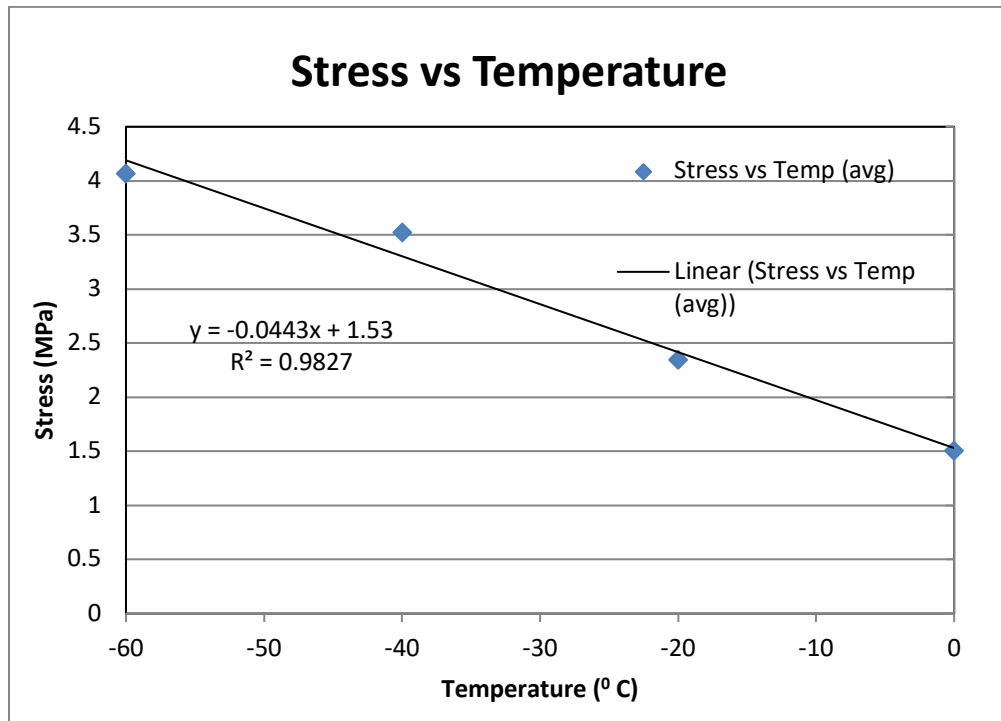
Figure 26: The effect of temperature on stress
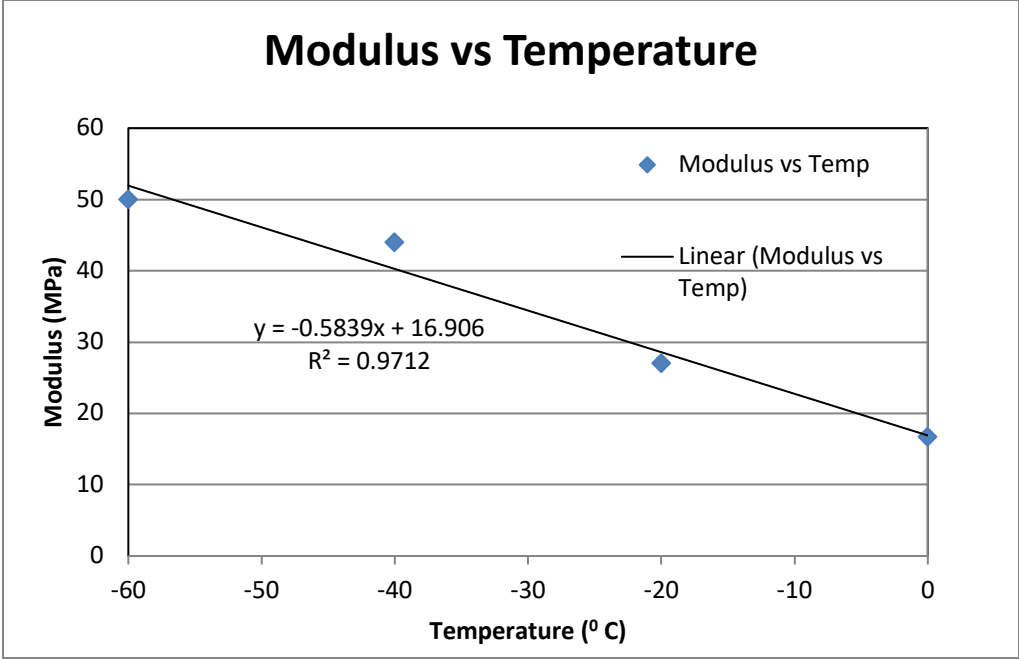
Figure 27: Effect of temperature on modulus
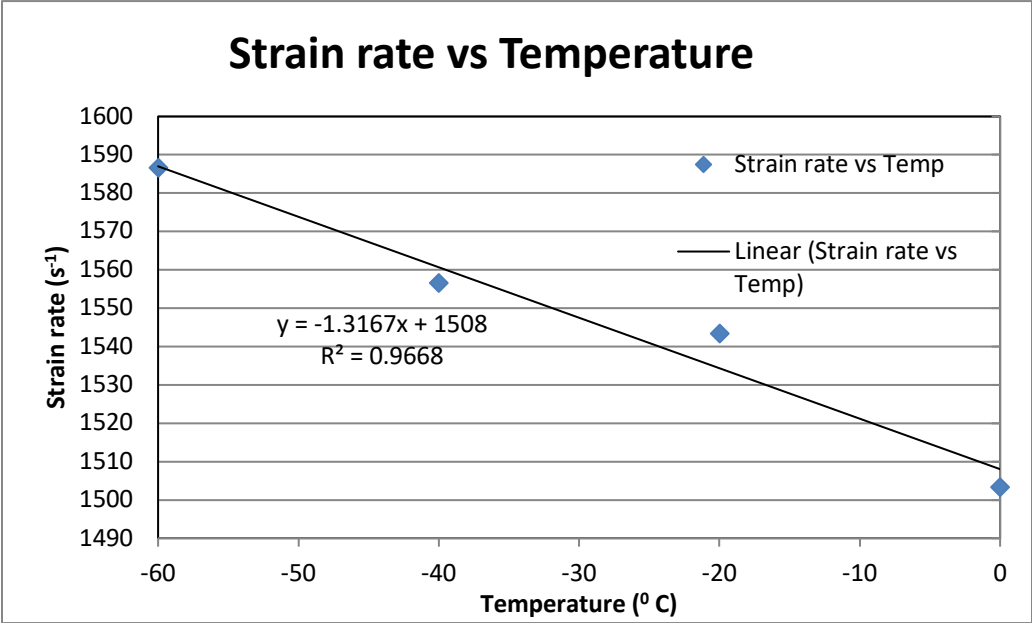
Figure 28: The effect of temperature on strain rate

As expected, the material stress increased as the temperature was lowered. In fact, the stresses and the strain at yield increased with decreasing temperature. This is consistent with other researchers that have investigated material properties as a function of temperature (Siviour et al., 2005). Meyers (1994) also agreed that most materials yield stress increases with strain rate and yield stress increase is more marked at lower temperatures. Maximum stress of 6 MPa was achieved in the specimen at an average strain rate of about 2000 s^{-1}. At room temperature, the maximum strain rate of approximately 2100 s^{-1} was attained for this material.

Utilizing solid pressure bars of 9.525 mm diameter and temperatures between 0^{0}C and -60^{0}C, the maximum strain rate of 2000 s^{-1} for the quick-recovery polyurethane foam was achieved. Testing with hollow pressure bars at room temperature yielded a maximum strain rate of 1400 s^{-1}. The sandwiched composite samples could not be tested on the 7.525 mm bars because it was not feasible to prepare samples of 7.9375 mm diameter, the size needed for testing such bars. Also, only dry samples were tested at Los Alamos National Laboratory because testing was done between 0 and -80^0 C and therefore testing fluid filled samples was not possible.

Figure 29 shows the dynamic modulus as function of strain rate of the different samples tested compared with the theoretical data obtained from Equation (19) developed with data from the modulus vs. temperature data and from the strain rate vs. temperature graphs. A simple relationship was developed to determine the modulus of this composite material as function of strain rate, as shown in Figure 29.
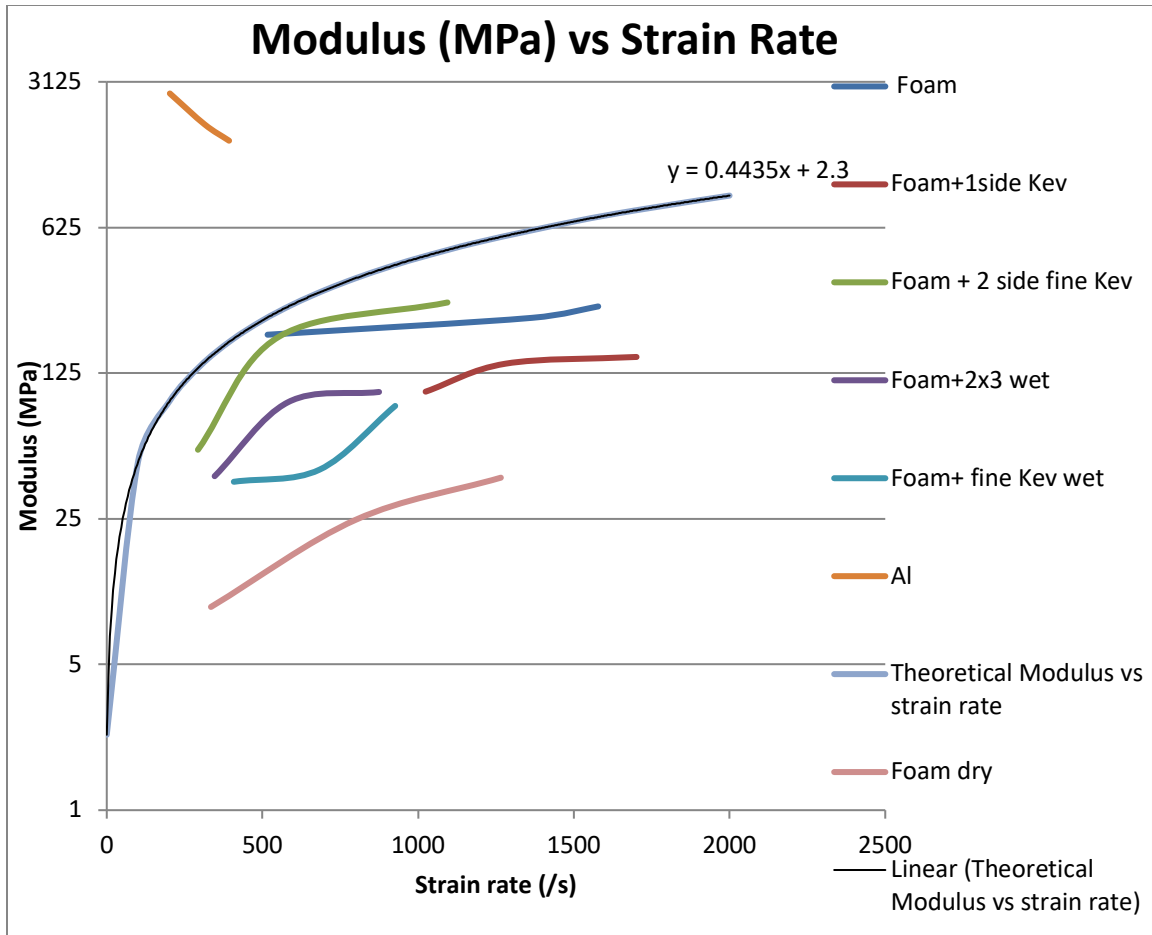
Figure 29: Comparison of the theoretical and experimental data

Additional tests were carried out on the foam samples on the SHPB at NMT to gather data to verify Equation (19) since Equation (19) was developed by testing the foam at temperatures of 0 ^{0}C to -60 ^{0}C. The foam sample was tested at breech pressures of 5, 10, and 15 psi corresponding to average strain rates of 731, 887, and 1260 s^{-1} respectively. The foam sample measured 25.4 mm in diameter and 4.7625 mm in length. Figure 30 below compares the theoretical data from Equation (19) and the actual test data of the foam specimen.
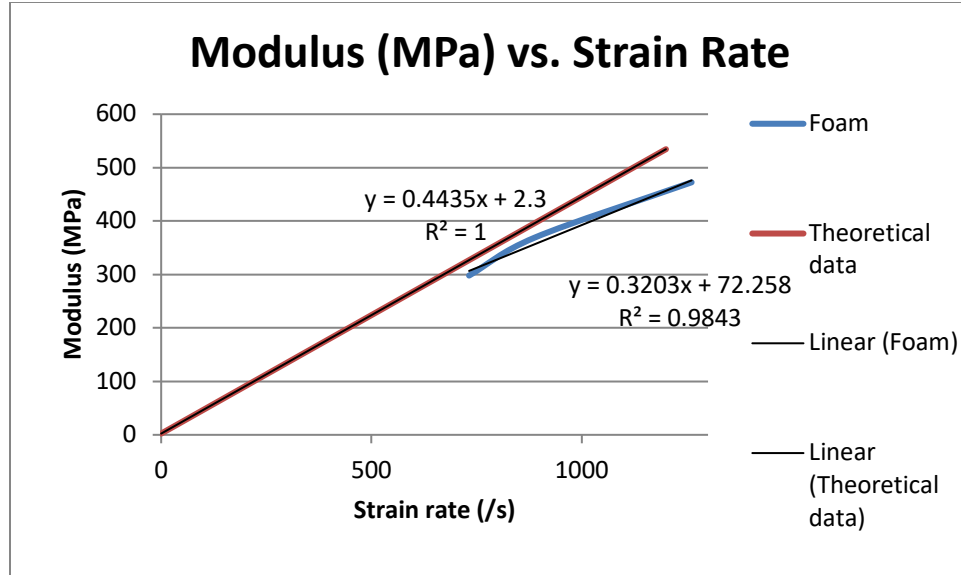
Figure 30: Comparison of the theoretical and experimental data

The experimental and theoretical data are in close agreement. This implies that tests done at low temperatures provided the valuable data that was used to develop Equation (19). The major differences between the two sets of data are the values of zero strain rates. According to Equation (19), zero strain rates yielded a modulus of 2.3 MPa, while the trend line for actual test data predicted a modulus of 72.258 MPa. The lower modulus at zero strain rates from Equation (19) resulted from the assumption that the trend of decreasing modulus with increasing temperature as shown in Figure 27 continued to room temperature. Also, the theoretical data reveals that the rate of increase in modulus with strain rate is 0.4435 while the experimental data shows the modulus increase at a rate 0.3203 with strain rate, as shown in Equation (20).

$$M = 0.3203\acute{\varepsilon} + 72.258 \tag{20}$$

61

Table 12 was developed using Equations (19) and (20) to show the percent difference and percent error between the theoretical and experimental data. It shows that Equation (19) can be used to determine the modulus of the 4.725 mm foam within about 20% error between the strain rates of 300 s^{-1} and 2000 s^{-1}.

Table 12: Comparison of the Theoretical and Experimental Data

Strain Rate (S^{-1}) $\acute{\varepsilon}$	Modulus (MPa) Theoretical M = 0.4435$\acute{\varepsilon}$ +2.3	Modulus (MPa) Experimental M = 0.3203 $\acute{\varepsilon}$ +72.258	Percent Difference (%)	Percent Error (%)
100	46.65	104.288	76.37	123.55
200	91	136.318	39.87	49.80
300	135.35	168.348	21.73	24.38
400	179.7	200.378	10.88	11.51
500	224.05	232.408	3.66	3.73
600	268.4	264.438	1.49	1.48
700	312.75	296.468	5.35	5.21
800	357.1	328.498	8.34	8.01
900	401.45	360.528	10.74	10.19
1000	445.8	392.558	12.70	11.94
1100	490.15	424.588	14.33	13.38
1200	534.5	456.618	15.72	14.57
1300	578.85	488.648	16.90	15.58
1400	623.2	520.678	17.93	16.45
1500	667.55	552.708	18.82	17.20
1600	711.9	584.738	19.61	17.86
1700	756.25	616.768	20.32	18.44
1800	800.6	648.798	20.95	18.96
1900	844.95	680.828	21.51	19.42
2000	889.3	712.858	22.03	19.84

The data from Table 12 was then used to produce Figure 31 which shows the percent error against strain rate. It is evident from this figure that strain rates between 100 s^{-1} and 300 s^{-1} have a high percent error. As mention earlier the constants in Equations (19) and (20) are quite different and may have influenced this error. However, these equations are valid for strain rates between 300 s^{-1} and 2000 s^{-1} and will serve as a starting point for developing the constitutive equation needed for characterizing this polyurethane foam composite under impact loading.
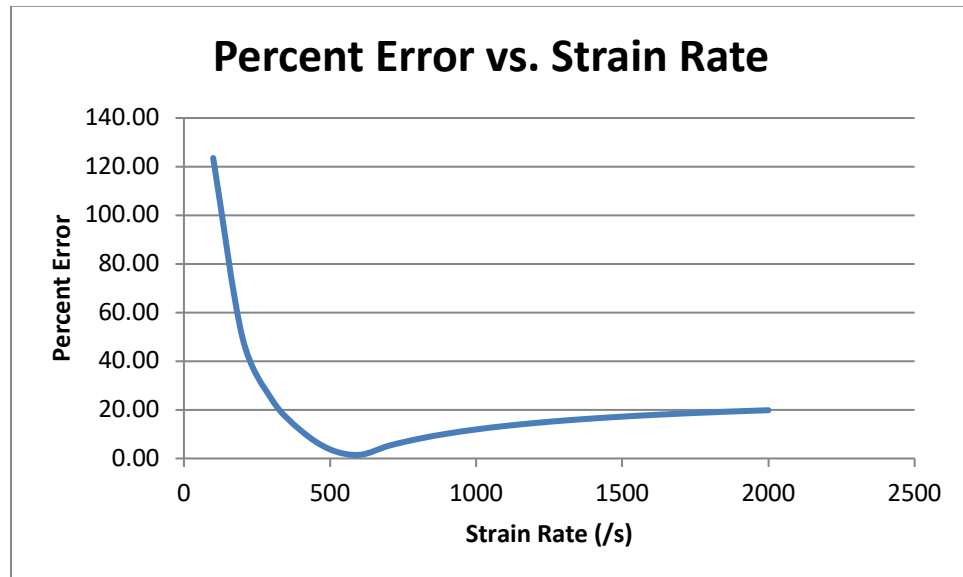
Figure 31: Percent Error vs. Strain Rate

CHAPTER 6 CONCLUSIONS

The necessary modifications were made to the SHPB apparatus at New Mexico Tech's laboratory and experiments were carefully conducted to determine the composite material's response to high strain rate loading. By increasing the impact velocities, the strain rates of the specimen were increased and the material exhibited an increase in dynamic modulus. The same trend was observed when the wet samples were tested. The strain rates obtained were between 100 s^{-1} and 1500 s^{-1} for 10.7 to 19.8 m/s impact velocities. Higher impact velocities could not be achieved on the current SHPB setup because it will produce yielding in the pressure bars and ultimately invalid data. According to the literature, smaller bars should be used for higher strain rates.

At low temperatures the yield stress increases with decreasing temperature. The low temperature tests resulted in the development of a simple relation that predicts modulus as a function of strain rate. This new composite developed by researchers at New Mexico Tech is a multifunctional material. Testing revealed it's excellence in acoustic dampening (Ghosh et al., 2007), induced convection during heating (Ghosh et al., 2010), and in this study, increased stiffness with increasing strain rates. The SHPB can be used to produce consistent data needed to formulate models of the constitutive properties of this new composite material.

CHAPTER 7 FUTURE WORK

Results of this research shown that the composite experienced an increased in stiffness with increasing strain rates between the range of 100 s^{-1} and 1500 s^{-1}. This is encouraging results and additional testing methods must be explored for a better understanding of this composite's behavior so that the range of applications for this material can be expanded. Also, additional tests will ultimately result in the development of constitutive equations that will predict this material behavior at high strain rates.

1. Further modification of the Split Hopkinson pressure bar can be explored with the aim of obtaining higher strain rates by employing smaller pressure bars and an output bar with a thinner wall. This modification will be intense since most parts of the apparatus will have to be replaced.

2. Other high strain rate testing methods should be explored to determine this material behavior at higher strain rate (See Meyers pg. 299).

3. Testing this material in an explosive environment can also provide valuable insight to its behavior at higher strain rates, therefore it should be pursued.

4. Preparing multi-layers samples, i.e. samples with different skin layers (e.g. Kevlar+Foam+carbon fiber) for testing under different loading conditions.

5. Taylor Impact test should be done for more in-depth investigation of the material's behavior.

REFERENCES

Beer, F. P., Johnston, E. R. Jr., DeWolf, J T. (2006) *Mechanics of Materials*. Fourth
Edition. Mc Graw Hill.

Chen, W., Lu, F., Winfree, N. (2002). High-strain-rate Compressive Behavior of a
Rigid Polyurethane foam with Various Densities. Experimental Mechanics,
Vol. 42, No. 1. Retrieved April 19, 2010, from the World Wide Web:
http://www.springerlink.com/content/b6357771u12w6760/fulltext.pdf

Chen, W., Zhang, B., Forrestal, M. J. (1999). *A Split Hopkinson Bar Technique for
Low-impedance Materials.* Experimental Mechanics Vol. 39, No. 2, June
1999.

Chen,W., Lu, F., Zhou, B. (2000). *A Quartz-crystal-embedded Split Hopkinson
Pressure Bar for Soft Materials*. Experimental Mechanics, Vol. 40, No. 1.
March 2000. Retrieved April 14, 2010, from the World Wide Web:
http://www.springerlink.com/content/61862830q4357p70/fulltext.pdf

Daniel, I. M., Ishai, O. (2006). *Engineering Mechanics of Composite Materials*. 2 nd
Ed. Oxford   University Press.

Frew, D.J., Forrestal, M.J., Chen, W. (2005). *Pulse Shaping Techniques for Testing
Elastic-plastic Materials with a Split Hopkinson Pressure Bar.* Society for
Experiemental Mechanics, Vol. 45. No. 2, April, 2005. Retrieved April 19,
2010, from the World Wide Web
http://www.springerlink.com/content/cn21377820130v33/fulltext.pdf

Ghosh, A. K., Morton, B., Birbahadur, N., Chavez, P., Sewal, E., Luders, I., Chavez, D. (2010). *A Novel Material for an Adaptive and Stealth Naval Plotform* (Rep. No. N00014-09-M-0005).

Ghosh, A. K., Williams, A. D., Zucker, J. M. Mathews, J. L., Spinhirne, N. (2007). *An Experimental Investigation into Acoustic Characteristics of Fluid-filled Porous Structures – A Simplified Model of the Human Skull Cancellous Structure.* Experimental Mechanics.

Graff, K. R. (1991). *Wave Motion in Elastic Solids.* Dover Publication.

Gray, G. T, (2000). *Classical Split-Hopkinson Pressure Bar Testing.* Mechanical Testing and evaluation, metals handbook. American Society for Metals.

Gray, G. T., Blumenthal, W. R. (2000). *Split Hopkinson Pressure Bar Testing of Soft Materials.* American Society for Metals, Vol. 8, 2000.

Harding, J. (1979). *Mechanical Properties at High Rates of Strain.* Department of Engineering Science, University of Oxford.

Humphrey, J. D. (2002). *Continuum biomechanics of soft biological tissues.* Retrieved December 04, 2009, from the World Wide Web: http://www.see.ed.ac.uk/~vkoutsos/Literature%20for%20Challenging%20Engineering%20Proposal/Continuum%20biomechanics%20of%20Soft%20Biological%20Tissues.pdf

Johnson, T.P.M., Sarva, S.S., Socrate, S. (2009). *Comparison of Low Impedance Split-Hopkinson Pressure Bar Techniques in the Characterization of*

Polyurea. Experimental Mechanics, 2009. Retrieved April 19, 2010, from the

World Wide Web:

http://www.springerlink.com/content/h561603387n02445/fulltext.pdf

Kaisers, M. A. (1998). *Advancements in the Split Hopkinson Bar Test*. MS thesis, VPI

1998. Retrieved December 07, 2009, from the World Wide Web:

http://scholar.lib.vt.edu/theses/available/etd-41998-

18465/unrestricted/ETD.pdf

Kolsky, H. (1949). *An Investigation of the Mechanical Properties of Materials at very*

High Rates of Loading. Retrieved October 11, 2010, from the World Wide

Web: http://iopscience.iop.org/0370-1301/62/11/302/pdf/0370-

1301_62_11_302.pdf

Kolsky, H. (1963). Stress Waves in Solids. Dover Publications Inc , pg. 87.

Kukureka, S. N., Hutchings, I. M. (1984). *Yielding of Engineering Polymers at Strain*

Rate of up to 500 s⁻¹. Int. J. Mech. Sci.,Vol. 26, 1984, p 617-623.

Lindholm, U.S., Yeakley, L. M. (1968). *High Strain Rate Testing: Tension and*

Compression. Experimental Mechanics, January 1968. Retrieved September

25, 2010, for the World Wide Web:

http://www.springerlink.com/content/1w656064t3113116/fulltext.pdf

Malvern, L. E. (1969). *Introduction to the Mechanics of a Continuous Medium*.

Prentice-Hall.

Mathews, J. (2008). Shock and Vibration Characteristics of a Bio-Inspired Structure

    under Blast Loading MS Thesis, New Mexico Institute of Mining and

    Technology.

Meyers, M. A. (1994). *Dynamic behavior of Materials.* Wiley.

Ninan, L., Tsai, J., Sun, C. T., (2001). *Use of Split Hopkinson Pressure Bar for off-*

    axis composites. International Journal of Impact Engineering 25, 2001.

    Retrieved December 12, 2009, from the World Wide Web:

    http://www.sciencedirect.com/science?_ob=MImg&_imagekey=B6V3K-

    423YKFN-5-

    4R&_cdi=5733&_user=1818435&_orig=search&_coverDate=03%2F31%2F2

    001&_sk=999749996&view=c&wchp=dGLbVlz-

    zSkzV&md5=922e617ee36230d5a952f012a7b92d53&ie=/sdarticle.pdf

Owens, A.T., Tippur, H.V. (2009). *A Tensile Split Hopkinson Bar for Testing*

    Particulate Polymer Composites Under Elevated Rates of Loading.

    Experimental Mechanics. Retrieved April 19, 2010, form the World Wide

    Web: http://www.springerlink.com/content/k17q0061711326l6/fulltext.pdf

Rogers Corporation, 2010.

    http://www.rogerscorporation.com/hpf/CT/PoronI/industrial_tech_info.htm

Sharma, A., Shukla, A., Prosser, R. A. (2002). *Mechanical characterization of soft*

    materials using high speed photography and split Hopkinson pressure bar

    technique. Journal of Materials Science. Retrieved April 19, 2010, from the

World Wide Web:

http://www.springerlink.com/content/5uj5ybyja924g379/fulltext.pdf

Siviour, C.R., Walley, S.M., Proud, W.G., Field, J.E. (2005). *The high strain rate compressive behavior of polycarbonate and polyvinylidene difluoride* . November 2005. Retrieved February 10, 2011 form the World Wide Web: http://www.sciencedirect.com/science?_ob=MImg&_imagekey=B6TXW-4HJ47YW-8-1X&_cdi=5601&_user=1818435&_pii=S0032386105015806&_origin=search&_coverDate=12%2F12%2F2005&_sk=999539973&view=c&wchp=dGLbVlb-zSkzS&md5=54967e8ff56b1bc23448c21696428fe2&ie=/sdarticle.pdf

Slaughter, W. S. (2002). *The Linearized Theory of Elasticity*. Birkhauser.

Song, B., Chen, W. (2004). *Dynamic Stress Equilibration in Split Hopkinson Pressure Bar Tests on Soft Materials.* Experimental Mechanics Vol. 44, No. 3, June 2004. Retrieved April 19, 2010, from the World Wide Web: http://www.springerlink.com/content/guh311h3j692p610/fulltext.pdf

Song, B., Chen, W. (2005). *Split Hopkinson pressure bar technique for characterizing soft materials.* Latin America Journal of Solids and Structures 2, 2005. Retrieved April 14, 2010, from the World Wide Web: http://www.lajss.org/index.php/LAJSS/article/viewFile/73/67

Walley, S. M., Field, J. E., Safford, N. A. (1991). *A Comparison of the High Strain Rate Behavior in Compression of Polymers at 300K and 100K*, J. Phys. (France) IV Colloq. C3 (DYMAT 91), Vol. 1, 1991, P 185-190.

Zukas, J. A., Nicholas, T., Swift, H. F., Greszczuk, L. B., Curran, D. R. (1982). *IMPACT DYNAMICS*. John Wiley & Sons, pg. 287-288.